TAMPEREEN TEKNILLINEN YLIOPISTO

ANTTI HÄNNINEN

ILLUMINATION DESIGN OF A MICROROBOTIC PLATFORM

Master of Science Thesis

Examiners: Prof. Pasi Kallio and
Prof. Hannu Koivisto
Examiners and Topic Approved in the Faculty of Automation, Mechanical Council Meeting 09.05.2012

ABSTRACT

TAMPERE UNIVERSITY OF TECHNOLOGY
Master's Degree Programme in Automation Engineering
HÄNNINEN, ANTTI: Illumination design of a microrobotic platform
Master of Science Thesis, 64 pages, 9 appendix pages
April 2013
Major: Learning systems
Examiners: Prof. Pasi Kallio and Prof. Hannu Koivisto
Keywords: Illumination, Paper fibers, Paper fibers, polarized illumination, polarized lighting

This thesis discusses the research on illumination design of a microrobotic platform. The platform is built to automatically perform individual paper fiber (IPF) and fiber bond measurements of a single bond in order to harvest understanding on paper strength. Mechanical and chemical properties of paper fibers are usually determined by bulk parameters or indirectly. Some fiber parameters have been characterized by using current tools, but new equipment is needed for higher yields and fiber-fiber bond measurements. Detailed individual fiber level measurement will provide important knowledge of individual paper fibers and bonds. This platform will also allow the possibility to perform and examine chemical manipulations on a single fiber or bond to improve strength properties of paper.

The platform is searching for the fibers using two cameras for a 3D-view of the fibers. It is equipped with two microgripper actuators to perform the grasping of IPF or two bonded fibers. The main task for this thesis was to improve the image quality by optimizing the fiber illumination for the two cameras. Secondary tasks were to check that this solution will also work in finding the actuators from the image and possibly allowing the bonded area measurements visually.

Evaluating the suitable illumination was performed by testing different types of illumination architectures and improving the most successful methods further. The first candidates were compared taking a set of sample images and calculating the fiber recognition performance for each.

Finally a new illumination module was designed to allow the use of special polarized backlight illumination inside the platform structure previously designed. This polarized illumination works using two crossed polarization filters behind and in front of the fibers to block direct light but letting through the light refracting and reflecting from the fibers thereby changing the type or direction of its polarization. The resulting image then has a good contrast between the black or dark background and the white or light coloured fiber targets.

TIIVISTELMÄ

TAMPEREEN TEKNILLINEN YLIOPISTO
Automaatiotekniikan koulutusohjelma
HÄNNINEN, ANTTI: Valaistuksen suunnittelu mikrorobottijärjestelmään
Diplomityö, 64 sivua, 9 liitesivua
Huhtikuu 2013
Pääaine: Oppivat järjestelmät
Tarkastajat: prof. Pasi Kallio, prof. Hannu Koivisto
Avainsanat: Valaistus, polarisoitu valo, polarisaattori, paperikuidut, paperi, kuitu, konenäkö, hahmontunnistus, digitaalinen kuvankäsittely

Tässä diplomityössä suunniteltiin valaistus mikrorobottijärjestelmään, joka on rakennettu yksittäisten paperikuitujen ja kuitusidosten lujuuden ja joustavuuden mittaamiseen. Järjestelmän on tarkoitus kerätä tarkkaa kuitutason tietoa paperista, jotta paperin lujuuteen liittyviä asioita voitaisiin ymmärtää paremmin. Yksittäisen kuidun tai kahden kuidun sidoksen mittaamiseksi tarvitaan uusia menetelmiä. Joitakin ominaisuuksia on pystytty tutkimaan kuitutasolla ennenkin, mutta tiedon kerääminen on näillä menetelmillä hidasta. Tässä työssä käsiteltävä järjestelmä mahdollistaisi automaattisen työnkulun. Näin ollen se pystyisi tuottamaan suuren määrän mittauksia sarjatuotantomaisesti.

Järjestelmä toimii etsien kahden kameran avulla kuituja näyteastiasta ja poimimalla niitä kahdella mikropinsetillä. Kameroista toinen kuvaa suoraa kuitujen yläpuolelta ja toinen sivulla viistosti. Tämä kuvausjärjestelmä pystyy paikantamaan kuidun sijainnin 3D-avaruudessa. Tämän diplomityön aiheena on parantaa kuvanlaatua kuitujen valaistuksen kautta. Lisäksi oli varmistettava uuden valaistusratkaisun toimivuus myös työkalujen kuten pinsettien kärkien etsimiseen, jotta kuiduista tarttuminen onnistuisi tarkasti. Työn aikana keskusteltiin myös mahdollisuudesta käyttää polarisoitua valoa kuitusidoksen pinta-alan mittaamiseen.

Valaistusmahdollisuuksien tutkiminen suoritettiin vertailemalla erilaisia valaistusratkaisuja teorian ja käytännön avulla. Valittiin kolme valaistusstrategiaa joiden suorituskykyä vertailtiin tarkemmin kymmenen kuvan näytesarjan ja kuitujentunnistusohjelmiston avulla. Parhaita valaistuksia pyrittiin parantelemaan entuudestaan ja valitsemaan yksi lopullinen ratkaisu, joka rakennettaisiin järjestelmään.

Testien jälkeen polarisoitu taustavalo lisäpolarisaattoreilla kameroiden edessä valikoitui parhaaksi ratkaisuksi. Tämä valaistus suodattaa suoran taustavalon pois ja päästää lävitseen vain kuituihin osuvan valon. Kuidut kääntävät niistä taittuvan ja heijastuvan valon polarisaation tietyn suuntaiseksi, jolloin vain tämä valo läpäisee kameran edessä olevan toisen polarisaattorin. Tuloksena on tummataustainen kuva jossa kuidut ovat hyvin valaistuja ja helposti eroteltavissa.

Tällaisen valaistusratkaisun sisällyttäminen aiempaan järjestelmän rakenteeseen asetti haasteita valaistusrakenteelle, joka oli suunniteltava järjestelmän muun toiminnan rajoitukset huomioon ottaen.

PREFACE

I would like to acknowledge the Finnish Funding Agency for Technology and Innovation (TEKES) and the Academy of Finland for their financial support of the projects (SmartFiber and FIBAM PowerBond), of which this thesis is a part of. I would also like to thank the Department of Automation Science and Engineering (ASE) of the Tampere University of Technology for offering me the opportunity to work with such interesting and challenging topic.

I am thankful to Prof. Pasi Kallio for the support and guidance throughout my thesis work giving me also a lot of freedom but also faith and objectives to cope through the sometimes challenging work. Also the atmosphere of my colleagues at the research group and the peer support they gave has to be appreciated because of the pressure relieving effect. MST group doctor students Pooya Saketi, Mathias von Essen and Juha Hirvonen deserve a special thank with the detailed help they gave me completing the tests and other tasks needed for the research. They also came up with the fundamental mechanical structure of the final illumination module.

Special thanks also to Timo Prusi from Production Engineering department and Heikki Huttunen from Signal Processing department for the expert knowledge on illumination and image processing algorithms.

Finally I would like to thank my close friends and family who supported me through the times when the progress felt difficult. Also my friends and floorball hobby should be addressed giving me the needed counterbalance during the stressing work.

Tampere, April 2013

ANTTI HÄNNINEN

CONTENTS

ABBREVIATIONS

ASE	Department of Automation Science and Engineering
AVT	Allied Vision Technology, company
DOF	Depth of Field in focus in Photography
FIBAM	Autonomous Microrobotic System for Manipulation, Stimulation and Characterization of Fibrous Materials, project
FOV	Field of View of a camera
IPF	Individual Paper Fiber
LCD	Liquid Crystal Display
LED	Light Emitting Diode
MATLAB	Matrix Laboratory, software
MST	Micro- and Nanosystems Technology
TEKES	Finnish Funding Agency for Technology and Innovation
PDMS	Polydimethylsiloxane
TUT	Tampere University of Technology
3D	Three-dimensional

SYMBOLS

d	Aperture diameter
d_i	Distance of focused image from a lens
d_o	Distance of object from a lens
f	Focal length
h_i, h_o	Height of the image and object
I	Intensity
m	Magnification
n_i	Refractive Index
p	Normalized probability
s	Exposure time
t	Histogram bin value
α	Angle of Refraction and Reflection
Θ	Angle between two polarizer filters
μ	Expected Value, Mean
ω_i	Probability
σ_i^2	Variance
ε	Exposure value

1 INTRODUCTION

The amount of investments into the development and research of microrobotic systems has been growing in recent years. Thus it has become possible to use them more often in technology applications also in practice. Commonly used applications of micro- and nanosystems lie in microbiology and microassembly. Other areas include nanoparticle manipulation and material characterisation. [1, 2]

Paper is composed of a network structure of fibers and other wood cells. The properties of these micro scale fibers and the bonds that form the network structure affect the quality of paper. Conventionally paper fibers are analysed and characterized through mathematical model estimation, or by using bulk parameters. Statistical analysis is performed to obtain the individual fiber bond level information [3, 4]. However, it is more accurate to perform the analysis from a bottom-up perspective. This is possible using individual paper fibers and paper fiber bonds and direct characterization of an individual fiber or a single bond [5, 6]. A system to perform such analysis automatically and with a high yield is the aim of the project that this thesis is a part of.

1.1 Project overview

This thesis was started as a part of the SmartFiber project, which was funded by TEKES, the Finnish Funding Agency for Technology and Innovation. After the end of SmartFiber project, the thesis was continued within the FIBAM project, funded by The Academy of Finland (Suomen Akatemia).

The goal of these projects is development of an automated microrobotic platform for characterization of individual wood fibers. The platform should be able to automatically grasp a single fiber or two bonded fibers from a sample pool. Grasping is achieved by a machine vision system controlling the actuators. The image processing algorithm finds the ends of a fiber and the micro gripper actuators will grasp them from both ends. The platform then executes manipulations or measurements of the sample in question. The automation of this workflow is essential because it would allow a high throughput for harvesting data. Currently the actuators are used by human manual control.

1.2 Objectives

The scope of this thesis is to choose a suitable illumination method for the machine vision system of the fiber platform. Improved illumination will make the automatic recognition of the fibers much easier as the previous illumination produced weak results. Currently the platform camera has an integrated coaxial illumination system,

which makes it possible to find the fibers from an image. However the image quality is not considered good enough to continue programming of the automatic fiber recognition software. Using software image manipulations to correct these weaknesses would not be the best solution because of the extra work and especially calculation time and complexity it would cause.

1.3 Thesis outline

The following chapters are organized as follows. Chapter 2 addresses the theoretical background of the thesis work. Chapter 3 explains the properties of the platform that is the subject of the work. In the next chapter, the methods and conditions of the illumination research are explained and test results from the early evaluations given. Design of the final illumination module is discussed in Chapter 5 and the results with this new system are evaluated in chapter 6. Chapter 7 includes the conclusions and some ideas for future works.

2 THEORETICAL BACKGROUND

In this chapter, the basic principles on the optics theory, illumination, machine vision principles are presented. This background theory knowledge will help to understand the decisions made and methods used in this thesis work during the research.

2.1 Optics

Light is needed for anything to be visually observed. The observer may be a human being or a machine vision system. Vision is based on illumination, reflections and recording of the reflected light. Light may be captured by optical devices and recorded by camera sensors. This section discusses the basic theory of optics needed in machine vision systems. The topics include reflection, refraction, lense systems and polarization of light respectively.

2.1.1 Reflection and refraction

Refraction means the phenomenon where a ray of light penetrates the medium in a certain angle and continues its journey inside the medium in question. The angle of incident is different from the angle of refraction because of differences in the two materials where light is traveling. Reflection happens when the angle of incident is larger than the critical angle of the medium in question. In this case, light bounces off the surface of the medium instead of penetrating it.

Law of refraction (Snell's Law) in optics states that light is reflected from a surface in the same angle it hits it

$$n_1 \, sin \, \alpha_1 \; = \; n_2 \, sin \, \alpha_2 \quad , \tag{2.1}$$

where α_i = the angle of incidence measured from the normal and n_i = the refractive index of a medium.

When a light of ray is reflected from a surface and continues its way as a single reflection, for example a mirror reflection it is called specular reflection. In such reflections the reflected image is maintained recognizable. The opposite of specular reflection is diffuse reflection. Diffuse reflection is a form of reflection where the incident ray is

reflected simultaneously in multiple angles rather only a single one. This is caused usually by substantial irregularities in the medium such as the fiber-like structure of paper for example. [6]

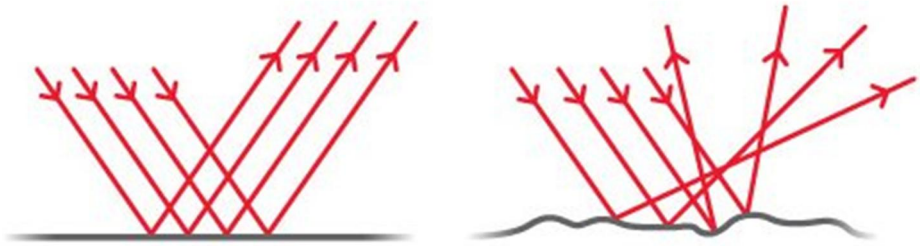

Figure 2.1 Specular and diffuse reflection [7]

Figure 2.1 illustrates how specular and diffuse reflections happen. The principles of reflection and refraction theory are important for this thesis. They help to understand how the illumination pattern may be manipulated. These illumination modifications may produce more desirable results of the subject and improve the image quality significantly from the default.

2.1.2 Lenses and lens systems

Lenses are the common tools used when capturing light to project an image for a camera to record. The target under inspection needs to be projected accurately enough in order to record the details of it. If something needs to be measured or inspected from an image, the resolution must be high enough to record the wanted details. This applies for the optical and lens system part as well as later for the image capturing device and media. The resolution of the whole system must be higher than the smallest detail the user wants to see in the resulting image.

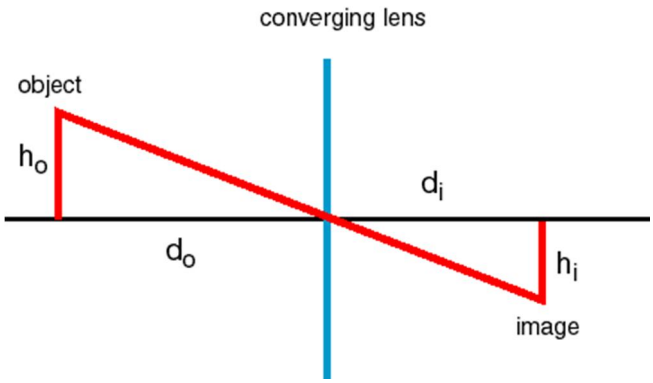

Figure 2.2 Thin lens projection of an object [8]

Accordingly to the figure 2.2, the magnification m of the optics can be derived from the pinhole equation:

$$\frac{1}{f} = \frac{1}{d_i} + \frac{1}{d_o} \tag{2.2}$$

$$m = \frac{h_i}{h_o} = -\frac{d_i}{d_o} \quad , \tag{2.3}$$

where f is the focal length of the lense and d_i the distance where the focused image of the subject is projected. h_i and $h_o$are the image and object sizes respectively and d_o is the object distance from the lens. [9]

When the working distance is kept constant, optics with a shorter focal length may capture image from a larger area than the ones with a long focal length. This imaging area is called field-of-view (FOV).

According to the Nyquist Criterion, the spatial resolution of the imaging system should be at least twice the smallest detail that needs to be measured. Together the resolution, magnification and FOV are some of the most important parameters when building a camera system for technology. Resolution and magnification decide how small and accurate details can be recorded while FOV is limit of the seen area.

The camera and lens system for the micro robotic platform in this thesis were previously selected for the project. However, it is important to understand the conditions they set for the system otherwise. In the thesis, it was also an option to make even large changes in the platform setup if it would be mandatory to achieve a satisfactory illumination.

These are the very basics of optical lens systems. Real optics used is more complicated but this theory is needed to understand some basics about how the optics may affect fiber imaging in this thesis.

2.1.3 Polarization

Light may be treated as a kind of electromagnetic wave. Simplest way of picturing such wave suggests that the orientation of the electric field is constant while magnitude and sign vary in time. This would be an example of linearly polarized light. Also other types of polarization exist, including circular and elliptic polarized light. Light is in fact almost always composed of different types of polarized and non-polarized components. Completely polarized or non-polarized light are only the very extremes.

There are techniques to change and manipulate the polarization type of light. Polarizer is an optical device, which turns natural light into polarized light. Figure 2.3 illustrates the action of a linear polarizer filter. These filters are usually sheets of polarizer material or ready-made polarization filters for photography or other imaging. Most common polarizers are either linear or circular in type.

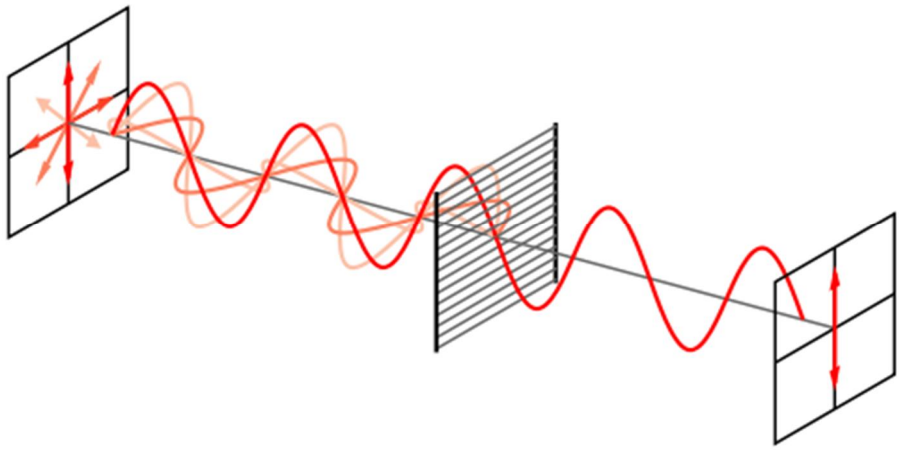

Figure 2.3 Randomly polarized light filtered with a wire grid type linear polarizer [10]

Polarizers are formed using four physical mechanisms: dichroism, reflection, scattering or birefringence. The polarizer selects a particular polarization state, which it lets through and block all the others with these mechanisms.

Scattering and reflection of light causes changes in the polarization. Scattering or reflected light may possess a certain form and direction of polarization. Using a polarizer it is possible to selectively block and let through such reflected and scattered light. This is often used in photography to block unwanted reflections from water, metal or glass surfaces. Polarizer may also make outdoor photographs more visually appealing by darkening blue sky by blocking certain polarized light components.

Using two polarizers on the same path of light, it is possible to gradually alter the amount and type of light passing through. When the polarizer directions are aligned (angle is zero), the two polarizers work almost as only one would be in use. The image is darker though. When the polarizers are rotated, more light is blocked. Finally, when the filters are diagonal (angle is 90º), almost all light is blocked. This second polarizer is also often referred as analyser as in Figure 2.4.

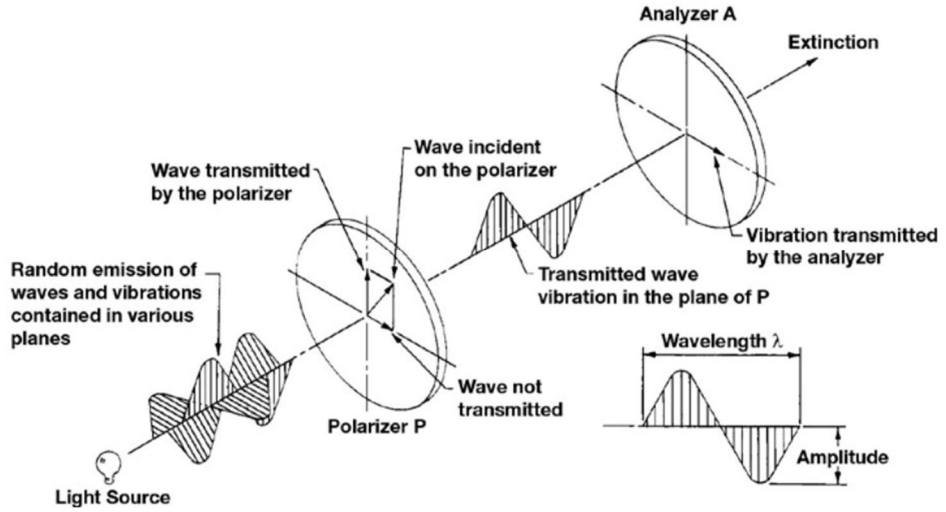

Figure 2.4 Two polarizer effect on the path of light [11]

The irradiance of this type of system with natural light passing through a polarizer and an analyser into some detector is given by Malus's Law:

$$I(\theta) = I(0)\, cos^2\theta \quad , \tag{2.4}$$

where $I(0)$ is the maximum intensity after the first polarizer, θ is the angle between the polarizers.

It should be noted that even an optimal polarizer alone lets through only half of the intensity passing through. However, if a subject of suitable material is located in between the filters, it may change the polarization of the light reflecting or refracting from it. This part of light will pass through the second polarizer and make the subject visible to the observer. If all the other light is filtered, this makes the subject stand out of the background. [9]

2.2 Machine vision

The process of observing a subject in machine vision is a multi-step process, which includes three main parts. First of them includes illuminating and optically observing a target as discussed earlier in this chapter. This section goes through the latter steps including the recording of the image and the image processing. The very basics of digital imaging and image pre-processing are explained first, then exposure and image segmenting in more detail. Optical properties of paper fibers are also shortly discussed.

2.2.1 Image acquisition

Digital images consist of a dot matrix where each dot or 'pixel' has digital numerical value describing the grayscale intensity value. To acquire an image after it is projected by the optical system, the photons have to hit the sensor pixels. A pixel of an image is

generated using the data from a sensor pixel or a group of sensor pixels. In colour cameras, a single image pixel may be built from four sensors, each of which is occupied with a colour filter. This construction is used in colour cameras and is called the Bayer matrix. In this thesis, a monochrome camera is used and colour information is not discussed in details.

As in the lens system in the previous chapter, also the sensor part of the system needs to have high enough resolution for the smallest details that need to be recorded in the image. The demands and solutions are explained in Chapter 3 as that research was accomplished earlier during the design of the platform.

2.2.2 Exposure

The amount of light a camera collects depends on the intensity of light falling on the sensor and the duration of this exposure also called shutter speed in cameras. The formula is following:

$$\varepsilon = Is \quad , \tag{2.5}$$

where ε is the exposure value, I is the image-plane illuminance (intensity) and s is the exposure time.

The intensity may be controlled apart from the illumination power (if controllable) also in the camera if the optics system is occupied with an adjustable aperture ring. By controlling the aperture diameter it is possible to limit the amount of light falling on the sensor. The aperture size also affects the depth of field of the final image: a larger aperture (more exposure) gives a shorter depth of field (DOF), while a smaller aperture extends the DOF. A longer DOF means that the subject area is in focus on longer length in front and behind of the focus spot.

The aperture sizes are also called F-stops or F-numbers. An F-stop is proportional to the ratio of the focal length f to the diameter d of the aperture. The smaller the F-number is, the larger is the aperture. [12]

$$F = \frac{f}{d} \quad , \tag{2.6}$$

where f is the focal length of the optics system and d is the aperture diameter. F is an F-number.

2.2.3 Segmentation

Image processing is used to extract information from a digital image. It has a key role in machine vision because image processing is used to choose and bring out the important information from image data. The image itself is not usable for technological applications directly, but the information such as shapes, patterns, colours can be extracted into numerical form for applications to use.

One of the most common and useful techniques in image processing is segmenting of an image in order to find certain subjects from the digital image produced with a camera or such. Images may be segmented by using the colour, intensity or texture information or more advanced methods of pattern recognition finding shapes for example.

Contrast in machine vision means the difference in the illuminance of two regions of an image that make the regions distinguishable from each other. In grayscale images, this simply means the difference of the gray value of these two regions. Contrast is the general term used to represent the properties which determine how an object or certain region may be segmented from a digital image.

A simple and most often used method of image segmentation is histogram-based thresholding. It means computationally selecting a threshold for the pixel intensities that will divide the image pixels to true or false (black and white) by comparing the intensities to the threshold value. [13]

Otsu's method

Otsu's method is a nonparametric and unsupervised method of automatic threshold selection for image segmentation. It is one of the very fundamental and important methods in image segmenting. It is used in machine vision when thresholding an image. The goal is location of subjects with certain intensity or colour value areas. The resulting image will have only two values black and white (0 and 1). Otsu's method is used to automatically perform optimal histogram shape-based image thresholding.

Otsu uses a statistical approach to minimize the intra-class variance in order to find the optimal threshold value. Otsu's method searches for the threshold, which minimizes the intra-class variance within class-variance that is defined as a weighted sum of variances of these classes.

$$\sigma_W^2 = \omega_1\sigma_1^2 + \omega_2\sigma_2^2 \tag{2.7}$$

$$\sigma_B^2 = \omega_1(\mu_1 - \mu_T)^2 + \omega_2(\mu_2 - \mu_T)^2 = \omega_1\omega_2(\mu_2 - \mu_1)^2 , \tag{2.8}$$

where ω_i are the probabilities of each class σ_i^2 the variances of them and μ_i the means. Indexes 1 and 2 denote the different classes, *W* intra-class and *B* inter-class.

The class probabilities and means of classes *i* are computed from the histogram. Using the left side values of the histogram, the values for class 1 are calculated:

$$\omega_1(k) = \sum_{i=1}^{k} p_i \tag{2.9}$$

$$\mu_1(k) = \sum_{i=1}^{k} i p_i \quad , \tag{2.10}$$

where *t* is the histogram bin value (or the middle value of the bin) and *p* is the normalized probability of the value. [14]

Similarly ω_2 and μ_2 can be computed using the right side values of the histogram for bins greater than *k*. The values are computed iteratively. The algorithm runs as following:

1. Compute histogram and probabilities for each intensity value
2. Set up initial values for the probability ω_i and mean μ_i
3. Go through each threshold value and update ω_i and μ_i and compute σ_B^2.
4. Maximize σ_B^2 to find the desired threshold

This yields a powerful algorithm, which is very commonly used and also implemented readily in MATLAB function.

2.2.4 Object properties

In this thesis, the objects are paper fibers, which are produced through pulping of wood mass. The fibers consist of cellulose, hemi-cellulose and lignin [15]. The size of an individual fiber is 16 – 70 micro meters in diameter and 0.8 – 4.5 mm in length. They are fibrillated, flat and twisting around their own axis, which makes them visually very thin in certain directions [15]. The physical size of the fibers creates standards for the imaging system, which have been taken into account before this thesis.

As discussed earlier, some materials have specific habit of changing the polarization of light scattering from it or passing through it. Also paper fibers possess this habit, which is a very important for this thesis.

2.3 Illumination

Illumination is an important part of a well working machine vision system. In many situations it might even be the critical factor concerning image quality. Correct illumination can make the problem very easy to solve computationally, compared to the situation, in which the software needs to correct the faults of poor lighting conditions. However, lighting itself is often not described very accurately in scientific papers that discuss machine vision systems. Often the lighting solutions are of a general type or ready-made products instead of carefully selected strategies. [16]

In order to obtain good quality images from certain conditions, the type of the illumination must be carefully chosen. Contrast should be maximized between the object that we want to examine and the background. The colour and the amount of light may be important, but so are the direction and the type of pattern of the illumination. Also some special techniques can be used to improve the contrast, such as polarized light and polarization filters.

This section introduces the different options and parameters in illumination design. These methods include choosing the pattern of the light, the geometry or direction of lighting and using certain filtering techniques.

2.3.1 Pattern

Extreme cases in the light pattern are collimated and diffused light. A mix of these two is often called directional light. Light may be diffused by using a diffusing filter in front of the light source. Also special diffuse dome systems exist. Collimated light is formed using certain type of optics to force the rays of light parallel to each other. It is used for special occasions such as precise silhouette size measuring with a backlight.

Directional and collimated light may be chosen in different situations. In certain situations, directional light causes wanted specular highlight reflections in certain situations. Often these reflections are also unwanted. Especially small bright peaks referred as hot spot reflections may distract machine vision algorithms. These intensive light peaks might also cause optical problems with the lens system or the optical sensor. A topographical peak can be found using illumination that causes reflections on uneven surfaces. Diffuse lighting causes less and fainter reflections. It is especially useful with bright field imaging of a reflective surface and whenever bright reflections are unwanted.

2.3.2 Geometry

The correct geometry of lighting can make subjects stand out from a scene. There are some methods for choosing the direction for the lighting so that it helps seeing a target

in an image. Multiple factors determine which illumination type is suitable for a certain problem. These include the properties of topography and reflectance of the subject and the background as well as the objectives of the illumination problem. In this section, the common illumination strategies are discussed to justify the decisions of the experimental part of this thesis work.

Bright field

Bright field illumination is the most common and perhaps the most intuitive group of illumination strategies. Light is directed straight to the subject from approximately the direction of the field of view of the imaging device. It is reflected back to the camera and the sensor is able to capture most of the reflected light. Figure 2.5 shows an example of this type of illumination.

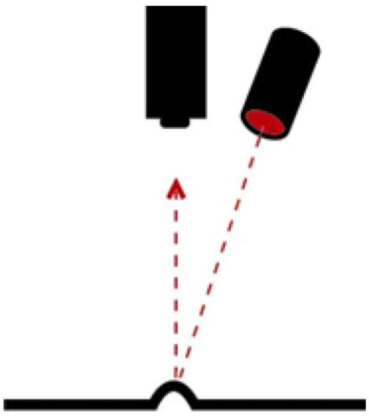

Figure 2.5 The principle of typical bright field illumination. [17]

Bright field illumination can be either full or partial bright field type. The light source can be coaxial or away from the optical axis of the camera.

Using bright field lighting often causes specular highlight reflections especially if the light pattern is not diffused. Depending on the problem this is either a positive or negative phenomenon. Bright field may be also diffused to decrease reflections [18].

For full bright field illumination, a diffuse dome is needed. It is a special kind of reflector used to produce an even illumination for the whole imaging area. The camera is located in the middle of the diffuse dome as in Figure 2.6.

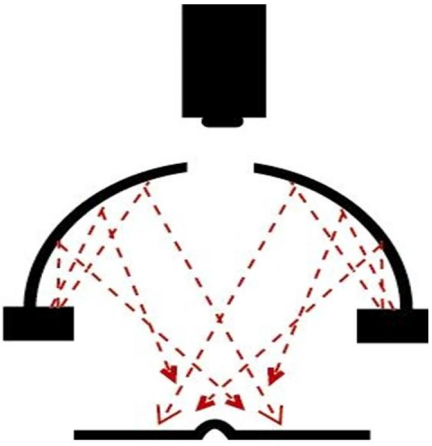

Figure 2.6 Diffuse dome illumination principle [17]

A ring light is an application of bright field illumination. It is often used to produce a smoother illumination with less specular reflections [19, 20]. Figure 2.7 is showing a usual flat diffuse bright field illumination scene. A typical ring light is an application of flat diffuse illumination.

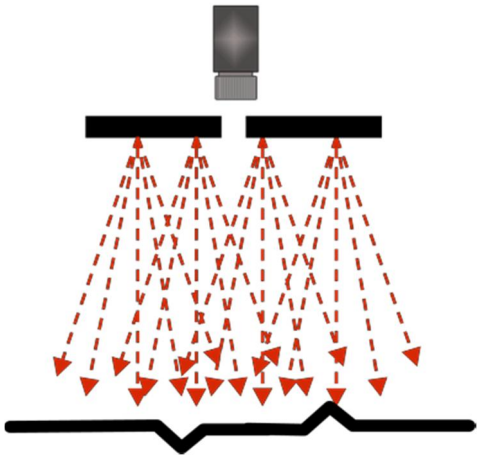

Figure 2.7 Simplified ring light illumination principle [17]

Another special application of bright field illumination is coaxial illumination. The light is sent out from the same direction as the camera is looking into the target. This is achieved by using a beam splitting mirror, which lets certain part of the light through and reflects rest of it. Using such mirror will enable directing the light from a source that is not on the axis of the camera, but is directed on to the same axis. This allows the camera to simultaneously register the light that is coming through the mirror. Coaxial illumination is useful for elimination of shadows caused by the subject. It is also useful with highly reflective surfaces and subjects. Coaxial illumination is used often in appli-

cations that examine specific reflective shapes and search for matching reflected patterns. The principle of coaxial illumination is shown in Figure 2.8.

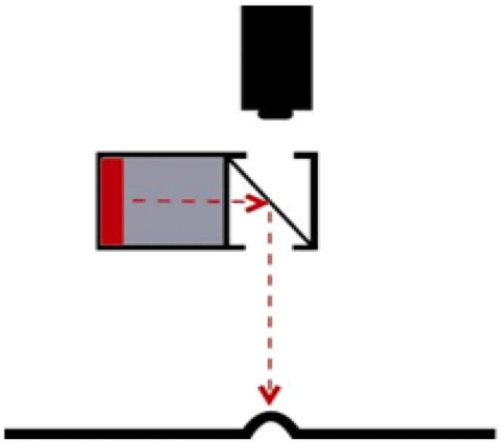

Figure 2.8 Coaxial bright field illumination [17]

Dark field

In certain cases, it is useful to direct the illumination oblique so that it does not reflect directly to the imaging device from the surface of the subject area that is seen by the camera. In such case, only the deviations on the surface come visible, as they reflect the light in a different direction – so that the camera can see the reflected light.

This type of illumination has been used in science and technology to inspect defects and other nonconformities on flat and reflective surfaces [21, 22, 23] and also in microscopy to emphasize topographical alterations in the subject. Figure 2.9 shows the basic idea of dark field illumination.

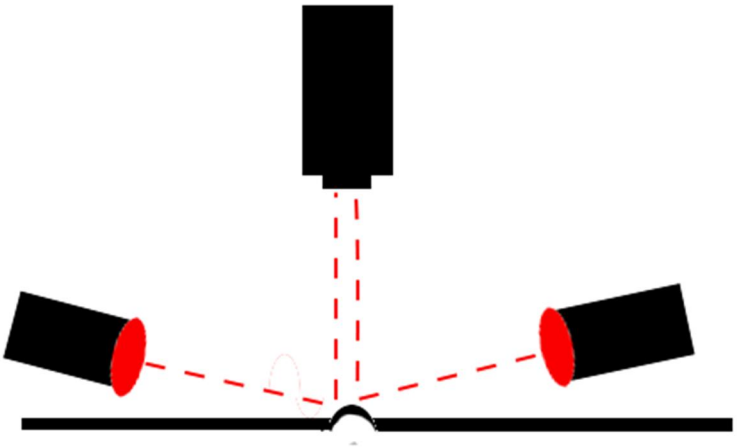

Figure 2.9 Dark field illumination. Redrawn from [17]

Backlighting

Backlight is used for either transparent subjects to observe the inner parts or non-transparent subjects. The camera receives the silhouette of the object, which can be used to extract information about the location and the size of a subject. Backlight illumination often uses diffused light. Sometimes a special collimated light source can be used for careful silhouette imaging and detail inspection. This will make the image more detailed for inspection of the small shapes of the subject. Backlight also makes it possible to see inside transparent materials. The principle of this illumination type is shown in Figure 2.10.

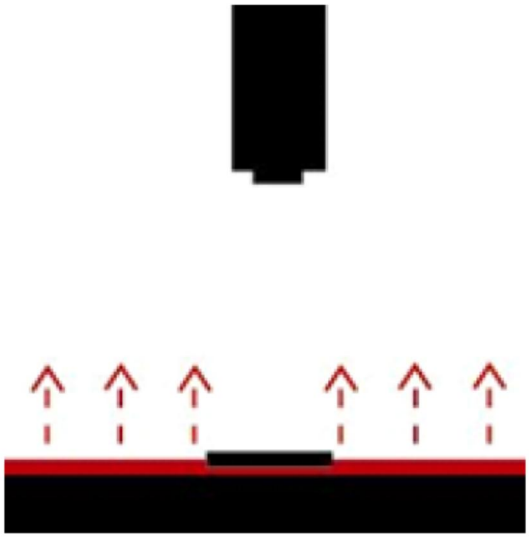

Figure 2.10 A simple scheme of backlight illumination [17]

2.3.3 Polarization techniques in practice

Polarizing techniques have been used in microscopy for some time [23]. Polarizing the light for illuminating microscopy subjects can change the vision of the subject drastically. Parts of the subjects may appear in specific colours when using polarized light. These colours expose differences in the properties of the subject and help in segmenting the image. The same technique is used in many applications such as stress analysis of industrial objects. [11]

3 MICROROBOTIC PLATFORM PROPERTIES

In the implementation of the chosen illumination techniques, some limitations are caused by the current design of the platform and system. Especially the actuators and their trajectory used for the manipulation of the fibers have to be taken into account when designing any new parts to be installed to the system. This chapter describes the main properties of the whole platform system and especially the factors that are limiting the development project of the illumination module.

3.1 Current state of the system

The platform itself is in a developing state in the laboratory of micro- and nanosystems research group in TUT. It is still more of a prototype and test platform than a final robot platform. Multiple small changes and modification plans were made to the system also during this thesis, but the principles of the operation remain the same as well as the main construction. This section describes the properties of the mechanical and optical hardware of the system as well as the current image processing software.

3.1.1 Hardware and space usage

Figure 3.1 shows the main architecture of the platform. The components are numbered in the image and explained here. Currently the platform is based on the platform floor (1) that is supporting the rest of the components. The actuators are built into a two story platform structure with four support pillars (2), roof plate (3) and the working plane (4) as the skeleton. The whole system can be easily transported for demonstrations outside the laboratory. A regular laboratory table supports the system.

A camera stand is attached directly to the platform floor (1) holding the camera and optics. The head of this stand holds the camera and the (upper) optics and is easily moved up and down by turning a rotating handle. During this thesis a second camera was added to the side to view the fiber samples in an angle. The purpose of this two camera setup is to create a 3D vision of the curled fibers for more accurate grasping of the fiber ends also in vertical Z-direction.

The two horizontal plates, which are fixed to the pillars, hold the actuators. The working plane (4) supports the XY-table (5) and a rotary table (6) on top of it. The rotary table has a sample cup on top of it. The XY-table is moved by the XY-actuators (8) below it. There is also a place for a micro force sensor on top of the XY-table for the flexibility measurements.

The roof plate (3) serves as a roof and supports the crane actuators performing the manipulation of the fibers. There are three micro gripper cranes (7) attached to the top plate from below.

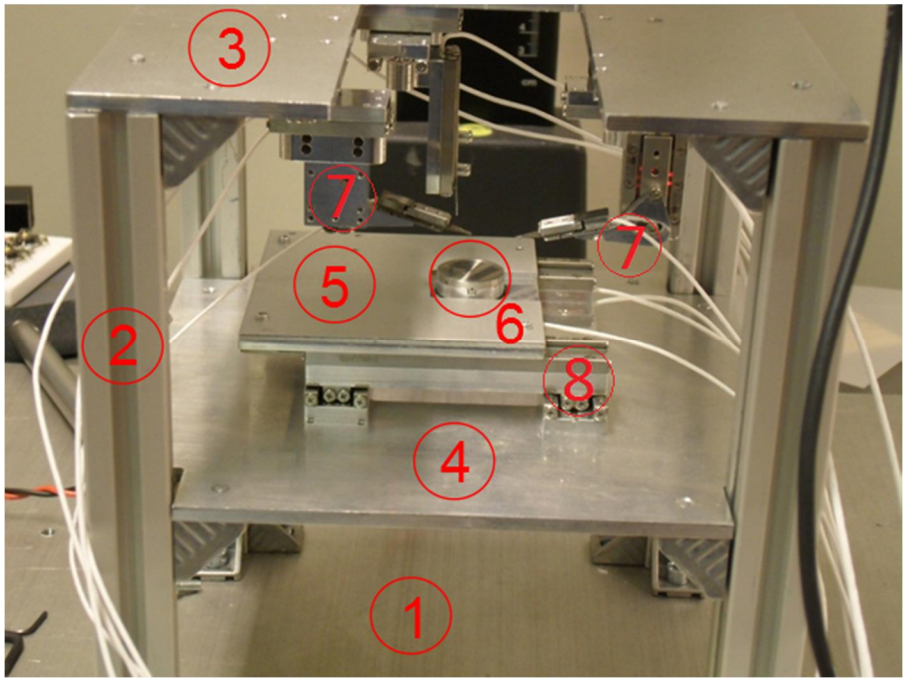

Figure 3.1 Previous design of the platform includes the platform floor (1), support pillars (2), roof plate (3), working plane (4), XY-table (5), rotary table (6), gripper actuators (7) and the XY actuators (8).

3.1.2 Imaging system

The platform imaging system was designed earlier but the solutions and the limitations of the system should be documented also in this thesis. The size and other properties of the fibers set certain demands for the performance of the optics, illumination and camera sensor. Further limitations are caused by the hardware settings of the imaging system.

The system is equipped with a Kaiser Fototeknik camera stand RS-1 and a suitable camera arm to hold the camera and optics above the fiber platform. The camera stand also gives an easy way of moving the camera in Z-axis position by simply turning a rotating handle. With the help of this Z-axis movement the camera may be focused in different distances if the height of the target changes.

To satisfy the demands of the problem, a 1/1.8 inch CCD sensor and a Navitar 12X zoom with a 0.5X lens attachment were chosen. The camera was chosen to enable a resolution of 1600 x 1200 pixels and a spatial resolution of 4.4µm. The working distance of this system is 165 mm and FOV is 27.58-2.28 mm^2. Magnification for this combination is 0.29X – 3.5X. Together these solutions fulfil the given requirements giving a suitable view of the fibers imaged [6, pp. 41-47]. Table 3.1 gives a summary of these components and their specifications or properties. The selected camera is Manta G-504B.

The second camera was added to the vision system in order to create a 3D-vision system for the platform. The aim is to allow accurate grasping of the fibers also in Z-direction.

A single camera observing the fibers from above is unable to extract the topology information of a fiber in the sample pool. is camera is currently a Sony XCG-U100. It is equipped with a Navitar Zoom 7000 Macro lens system with motorized aperture and zoom. Focus is currently manual. This camera is shown on the left in Figure 3.2.

Table 3.1 Vision system components and their properties

Component	***Specifications and properties***
Manta G-504B camera (top)	1/1.8 inch CCD sensor 2452x2056 pixel resolution, 3.45 µm spatial resolution
Sony XCG-U100 Camera (side)	1/1.8 inch CCD sensor 1600x1200 pixel resolution, 4.4 µm spatial resolution
Kaiser RS-1 with a camera arm (top)	Moves the top camera along Z-axis
Manfrotto 055 camera stand with a 804RC2 head (side)	Side view camera stand. Height, positioning, direction and angular 2-way rotation of the camera
Navitar 12X zoom, 0.5X attachment	27.58-2.28 mm^2 FOV, 165 mm working distance 0.29X-3.5X magnification Motorized zoom and focus
Navitar Zoom 7000 Macro lens system	18-108 mm focal length 183 mm x 142 mm field of view at 18mm 31 mm x 24 mm field of view at 108 mm 6X magnification 130 mm working distance Motorized aperture and zoom Manual focus

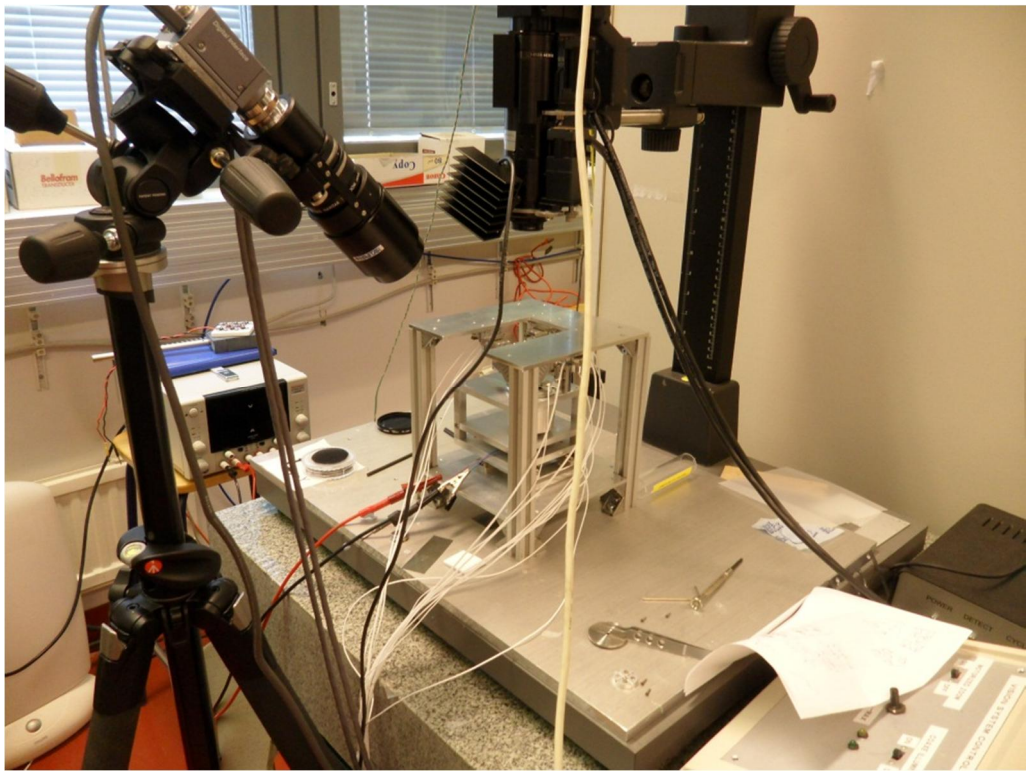

Figure 3.2 Platform and the vision system of two cameras

3.1.3 Illumination

At the time this thesis was started, the micro robotic system was utilizing a coaxial illumination system integrated to the optics of the top view camera. The manufacturer is Navitar and the model Led Coaxial Illumination WHITE 5500K 4.8 Watt. The coaxial lighting performs weakly because of the limited illuminated field of view it produced. This illumination could only produce light for an area much smaller than the sample pool is. The contrast of the images was weak and could also be improved significantly.

For some demonstrations, a general diffused lighting or even ambient lighting resulted in better images. However, the fibers could not be recognized accurately or reliably from the sample images. The platform usage needed a human operator to grasp the fibers using tele-operated procedure [6]. Figure 3.3 shows an example of the performance of this coaxial illumination system.

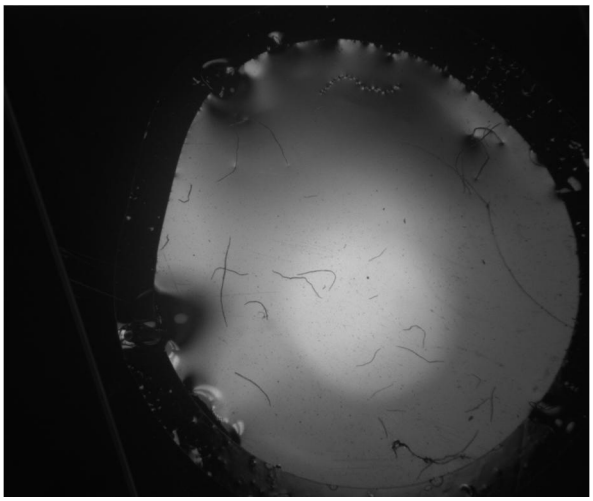

Figure 3.3 An image showing the performance of the coaxial bright field illumination built in to the platform top camera

3.1.4 Fiber sample pool

In the previous design an aluminium cup is used for storing the sample – fibers and water. During the tests for this thesis, also backlighting of the fibers was necessary. During the prototyping and testing of the illumination methods, a microscope slide glass with a 100 micro meter high ring made of polydimethylsiloxane (PDMS) and later plastic sticker as used instead of the aluminium cup. The ring was attached to the slide and was used to simulate the edge of the rotary table cup used in the previous platform version. The purpose of this cup edge is to keep the fluid surface maximally flat when the sample liquid with the fibers is put on the rotary table. After the sample is injected into the container some of the redundant water is sucked back. This forces the liquid surface stay flat and causes less reflections and topographical variance. Figure 3.4 shows the plastic ring attached to a microscopy slide together forming the sample pool.

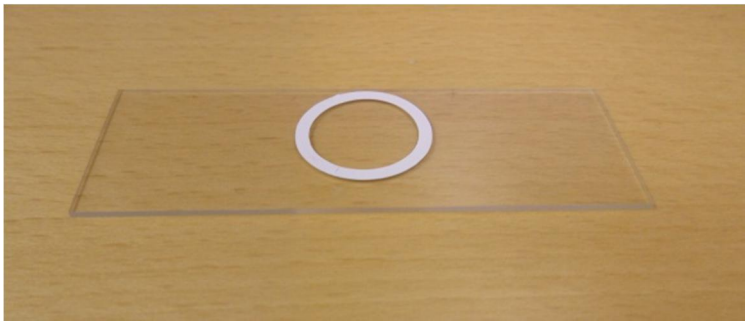

Figure 3.4 The microscope slide with a plastic sticker ring used for the tests to simulate the fiber sample cup

3.1.5 Software and hardware parameters

The camera stand settings, aperture and focus settings, illumination power and ambient illumination adjustments as well as imaging software settings, create changing parameters that might cause disturbance in image quality. These settings are important when creating a data set of images that need to be comparable with each other, as it is the quality of the illumination that is under research, not the imaging software.

While doing this thesis, most of the parameters remain at least relatively constant. The subjects as well as the cameras stay in comparable positions and distances and in same room. Thus, also the focus, location of cameras and ambient illumination stay comparable. The aperture settings of the cameras might need minor adjustments caused by lightness of the room or such. Most of the hardware side changes are after all compensated by the imaging software.

The cameras are controlled by individual computers and software programs. During this thesis, the side camera ran on a Linux computer using Coriander (version 2.0.0) while the top camera was ran on Windows using a Navitar 2-axis motor controller software (version 2.07). The Navitar software only controlled the fine focus of the top camera, while Coriander was used to control the focus, zoom and aperture settings for the side camera. It had also settings for controlling the image quality such as brightness, exposure, sharpness, gamma, shutter, gain. Similar settings are found in the Allied Vision Technologies (AVT) Unicam (Version 1.2.0.2) used with the Windows computer.

For the images in this thesis, these settings were left default in almost all cases. During the first tests, a few problematic images needed manual exposure setting or shutter speed control to result in a reasonable image. These cases included the coaxial illumination tests, which were special because of the uneven light distribution. During the larger data sets were produced, these parameters were set to defaults, thus all the numerical results presented in the thesis are shot with default settings. Changing them might cause different results and cause the test to be incomparable with the results of this thesis. The parameters of the two programs are documented in Table 3.2 and Table 3.3.

Table 3.2 Image settings for Coriander software of the side camera

Coriander	
Brightness	1024
Auto exposure	*ON*: 512
Sharpness	4
Gamma	0
Shutter	200
Gain	0
Trigger delay	*OFF*
Pan	12
Tilt	16
Filter	0

Table 3.3 Image settings for the AVT Unicam software running the top camera view

AVT Unicam	
Shutter	*Auto*, absolute
Gain	0
Target gray level	50
Brightness	0

4 ILLUMINATION RESEARCH

As the selection of the illumination setup for fiber imaging was not straightforward, a practical way of finding a suitable illumination was chosen in this thesis. Different lighting constructions and solutions needed to be compared against each other. The resulting images were evaluated to find out, which solution should be implemented. The theory of Chapter 2 was used to create the test methods and choosing the illumination methods used for the comparison. This chapter explains the conditions and methods used in the research and the illumination strategies taken into the comparison. Finally the selected illumination is built into a prototype and the results discussed.

4.1 Conditions and methods

The conditions, equipment and the image processing software used for the illumination research are explained in this section. First the general conditions are described and then the methods of preliminary testing of illumination are discussed. Later the actual test methods and the used image processing software are explained.

4.1.1 Preliminary tests

In the first phase, test images were taken with several different illumination setups. The different lighting options were only compared by visual overall inspection of the images by eye. Figure 4.1 shows examples of the performance of these early test samples.

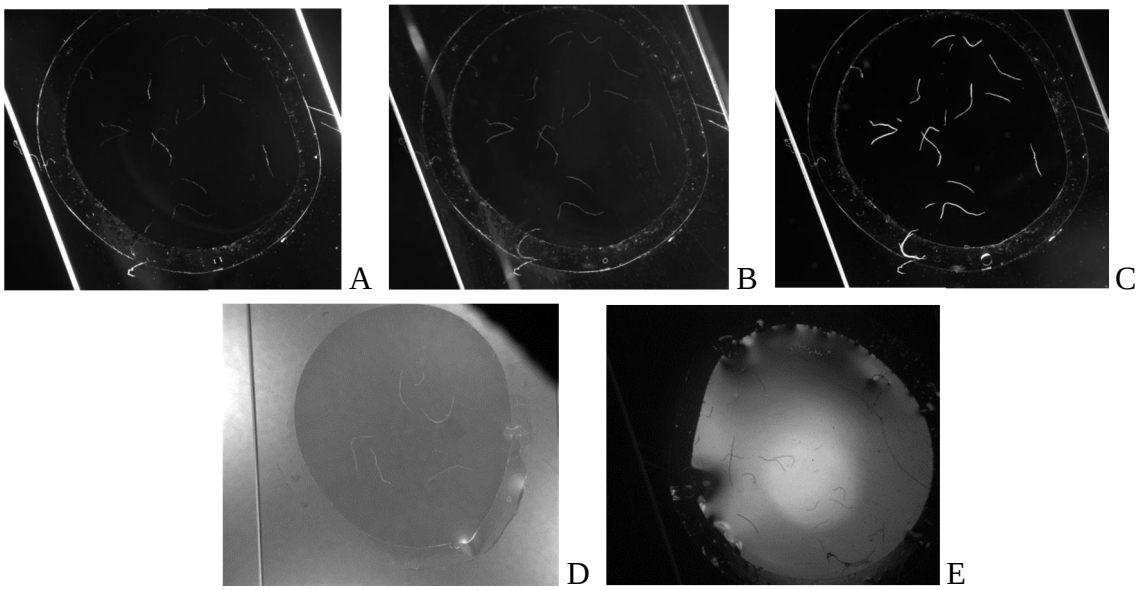

Figure 4.1 Early test samples

The Illumination techniques tested were: ring light (dark field, A), LED array dark field (B), polarized illumination (C), backlighting (D) and coaxial illumination (E). The latter two could be quickly disqualified because of lack of contrast, reflections and non-uniform illumination in the images. Those faults resulted in overall weak image quality and visibility of the fibers.

Because of limited time and resources in this thesis, only the current top three illumination techniques were qualified for further research, which would then result in choosing the final illumination to be built into the platform. The top three qualified illumination techniques were chosen to be dark field ringlight, LED arrays for dark field illumination and polarized backlight illumination. Figure 4.2 demonstrates the performance of these three configurations. The more accurate results are discussed in the next chapter.

4.1.2 Evaluation methods

After comparing the first results of different illumination schemes, three best options were chosen for development. The best configurations would be emended one by one and then compared more carefully against each other with a larger sample set of images. The sample set would be a set of 10 images taken of the microscope slide holding a random amount of fibers randomly aligned on the slide. Each sample usually held more than 10 fibers. This procedure and research would lead to an improved way to illuminate the paper fibers.

In the beginning, it was a difficult to find the best ways to measure the software performance in each illumination. First some mathematically complex approaches such as the Chernoff information filter, neural networks, and different pattern recognition algorithms were considered to compare the image quality and the performance of the illumination. After discussion with other research group members, a more practical and mathematically simple approach was found more relevant in a problem such as this.

The number of correctly recognized fibers using the platform software was compared with the number of total individual fibers in each image. By calculating this ratio for each image, a simple scalar is obtained to describe the success of the illumination. To give a more comparable result, the fibers that are only partly recognized are counted in different category. These counts appear in the column named ‘Ratio’ in the tables of this section. The fibers that interfere with each other in the image are disqualified because they cannot be reliably grasped and measured and would cause problems later in the function used to search the fiber ends.

4.1.3 Fiber recognition software

The future goal of grasping and manipulating the paper fibers automatically demands the recognition of individual fibers from the images taken by the both cameras used in the platform. The group has earlier developed software for this image segmentation.

This software is still under research as also the used images are changing during this thesis work. The MATLAB code of the main program is presented in Appendix B. The main properties are discussed in this section.

The fiber image is segmented into two classes by the software; fibers and the background. This segmentation is performed using simple threshold with Otsu's method explained in Section 2.2.3. Often, the recognized fibers appear with some gaps after the applications first actions. Therefore, the threshold image is morphologically filtered to remove minor gaps splitting them in two. The smallest shapes segmented as a fiber are discarded by filtering.

A correctly recognized fiber needs to consist of long enough part of a fiber. There is a parameter for a minimum length (in pixels) in the program that may be adjusted. The minimum length depends on the hardware restrictions of the micro grippers of the platform.

After the segmentation phase, the program will skeletonize the thick fibers and search for the endpoints from where the fiber should be grasped. This means the fiber should not have multiple branches, thus also the fibers crossing each other in the sample pool are discarded. Stacking of fibers is a common phenomenon and will result in many discarded sample individuals.

For the illumination research of this thesis, the program was modified slightly. A possibility to discard any information outside the sample pool ring was added to the program. The result of this selection is shown in Figure 4.2. The mask blocking the outside of the sample pool is also used in the threshold calculation to prevent any distortion from the 0 areas outside.

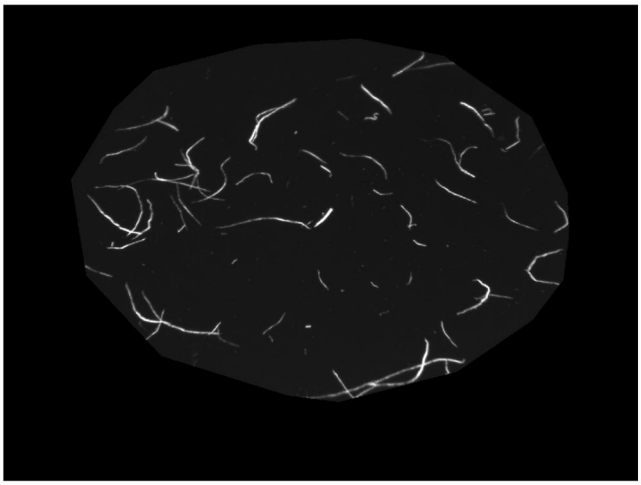

Figure 4.2 A sample image from the software used for the fiber calculations

The final segmentation results from the software would look like in Figure 4.3 Gray background between the fibers is removed. The next steps in locating the grasping points would be to discard the crossed fibers, skeletonize the potential ones and then find the ones with only two unique endpoints [24].

Figure 4.3 Threshold result from the previous fiber sample

4.2 Illumination configurations

The three most promising illumination configurations were chosen for further evaluation in order to find the most successful to implement into the platform. The test configurations were very simple setups and are explained in this section.

All of these configurations were tested with a platform duplicate stripped of the actuators. The duplicate is of the same size as the actual platform and is built with same support pillar architecture. The construction is seen in several images of the illumination setups later in this section. The fibers were set on the top level instead of the normal height of the sample pool, but this was compensated by lifting the camera level higher to maintain comparable focus and zoom parameters. This duplicate also had a built-in LED illumination that is explained at the section discussing polarized illumination testing.

4.2.1 Dark field ring light

A ring light may be utilized to form dark field type of illumination by positioning and directing the illumination appropriately. For the fiber platform this was simple because of the narrow FOV of the cameras. The light enters the field of view from relatively low angle, in this case producing dark field type of illumination as shown in Section 2.3.2.

A ring light previously manufactured in the MST research group at TUT was used. It is formed of metal rings as the skeleton. Total of 16 Lumiled Luxeon Star LEDs are attached to the outer ring on regular distance of approximately 28mm. The distance of

opposing LEDs is approximately 142mm. Half (8) of the LEDs are Lambert White and half Lambert Red because of the earlier use of them in a thesis work [25]. The thesis also goes through the design of the ring light in more detail.

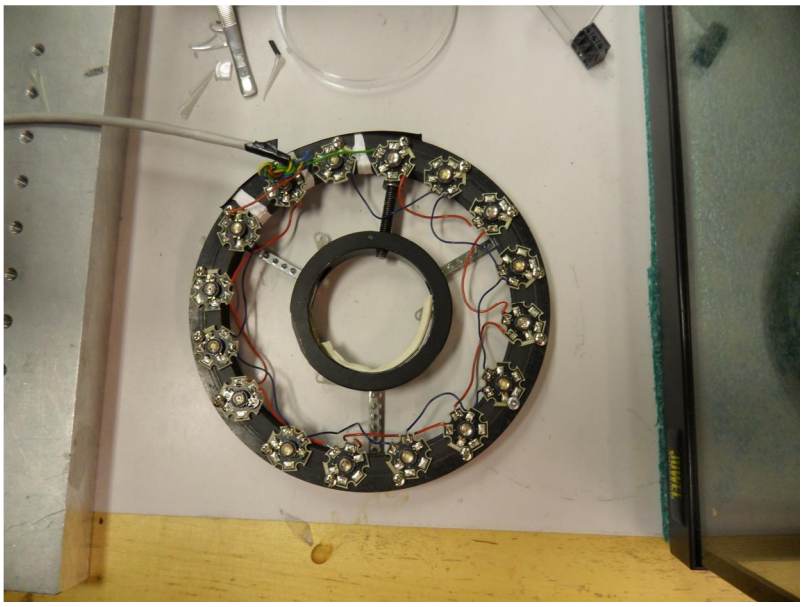

Figure 4.4 Image of the ring light in the laboratory

The ring light unit is shown in Figure 4.4. It is attached to a laboratory standard holding it approximately 15 cm above the top of the platform. The setup pictured in Figure 4.6 shows the vision system and the ring light illumination. This positioning illuminates the fibers in an angle that makes the illumination dark field in nature. Light is hitting the sample pool in a low angle and the reflected illumination is not captured by either of the cameras. The fibers however do reflect the light also in to the cameras and makes them stand out of the background.

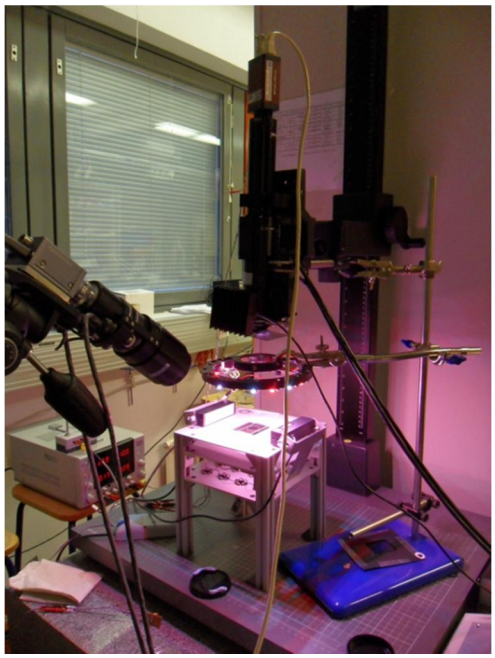

Figure 4.5 Test setup used for dark field ring light illumination

4.2.2 LED array dark field

Linear LED arrays used in the research, were LATAB lighting LED arrays (type SAH4 2122 or similar) equipped with a diffusor filter in front of the LED's to produce even illumination. There are two lines of red LED's and the array front is occupied with a diffuse filter. Two of these arrays were attached to the platform surface to left and right side of the subject, 5 centimetres away from the side of the microscope slide glass holding the fibers. The light sources were borrowed from Department of Production Engineering of TUT. The principle of this illumination architecture was also produced in cooperation with this department [26]. The setup is seen in Figure 4.7 below.

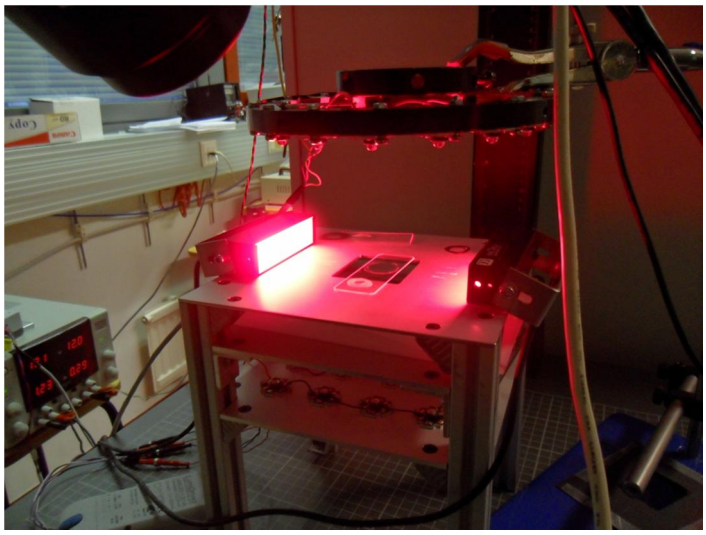

Figure 4.6 The LED array dark light illumination test setup

4.2.3 Polarized backlight illumination

The most complex of these illumination setups was the one used to demonstrate polarized illumination. An illumination test bench previously produced in the MST group was used to create the backlighting. This test bench was constructed with a similar skeleton as the actual fiber platform - four support pillars hold three planes. The lowest plane is equipped with a matrix of 16 green high power LEDs similar to the ones used for the ring light in Section 4.2.1. The next plane was used to hold a diffuse filter taken out of an LCD (Liquid Crystal Display) screen as well as the first polarizer. The highest plane held the microscope slide and the sample fibers.

The location of the diffuse filter is 5 cm above the LEDs. A piece of a linear polarization filter slide was used as the lower polarizer and was located on top of the diffuser. The top polarizer was a Kood linear polarizer filter, typical for photography use. It was supported by a laboratory standard. Figure 4.7 illustrates the setup used for this illumination strategy.

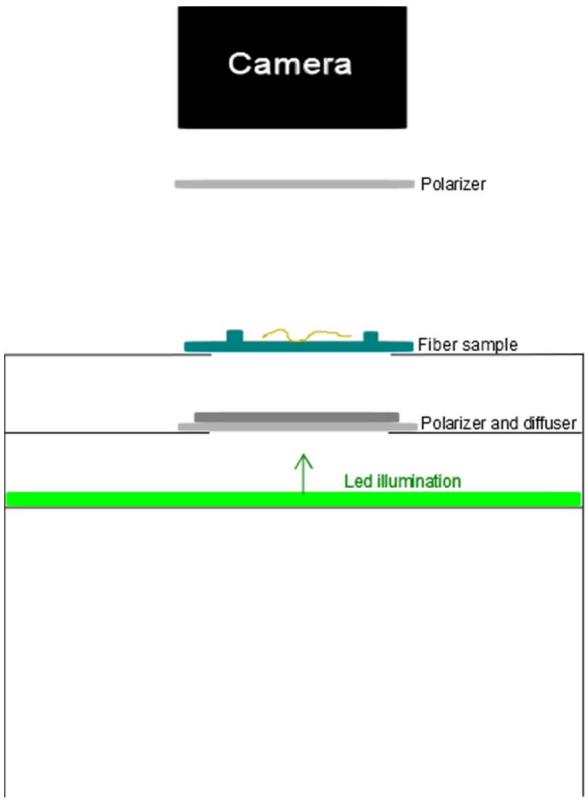

Figure 4.7 A scheme of the illumination setup

The fibers were set the on the sample pool glass, which was located 3 cm above the filters. A second and similar filter as the other top polarizer was also attached in front of the side-view camera. Figure 4.8 shows a photo of this whole setup. The cameras are seen at the top (middle) and on the top right as black objects.

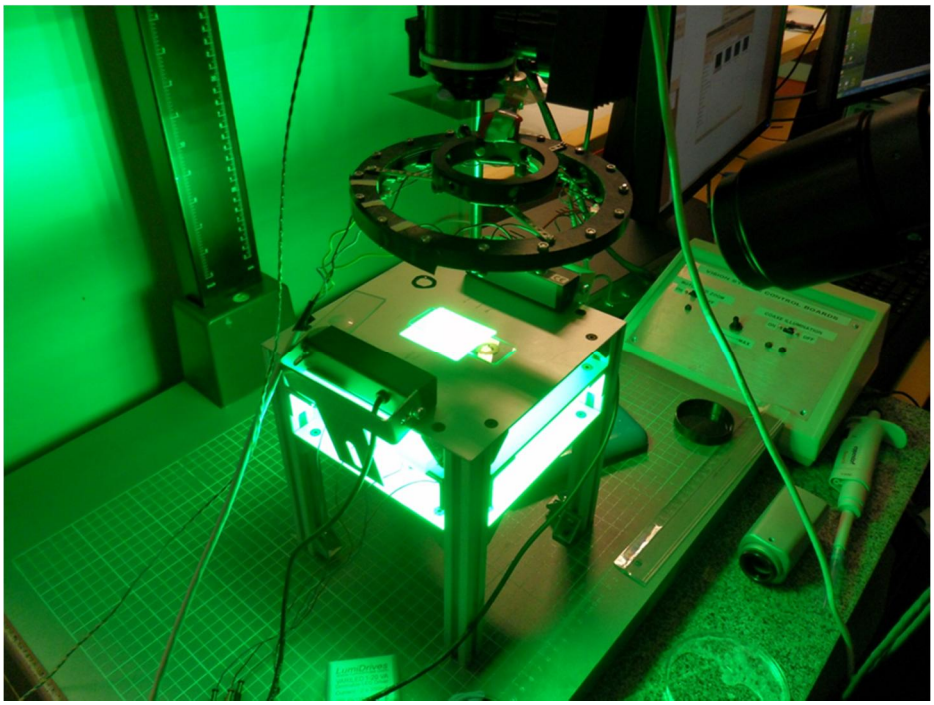

Figure 4.8 Polarized backlight illumination test setup

4.3 Test results

This section explains the testing and results of the illumination research. Sample images are shown of each setup and the fiber count results are given in table forms. Each sample image is segmented with the software introduced in Section 3.1.5. The number of total fibers is counted from each sample image and compared with the found fibers after segmentation. Completely and partially recognized fibers are counted in their own columns. The ratio column is a ratio of these two columns compared with the total amount of the fibers in the original image. On the bottom row, the cells represent sums of the columns except for the total ratio, which is calculated as the ratio of these bottom row cells as on previous rows.

4.3.1 Dark field ring light

An example of the image quality of dark field illumination with the top camera is shown in Figure 4.9. The fibers stand out of the dark background and neither the background nor the glass slide shows distractive reflections.

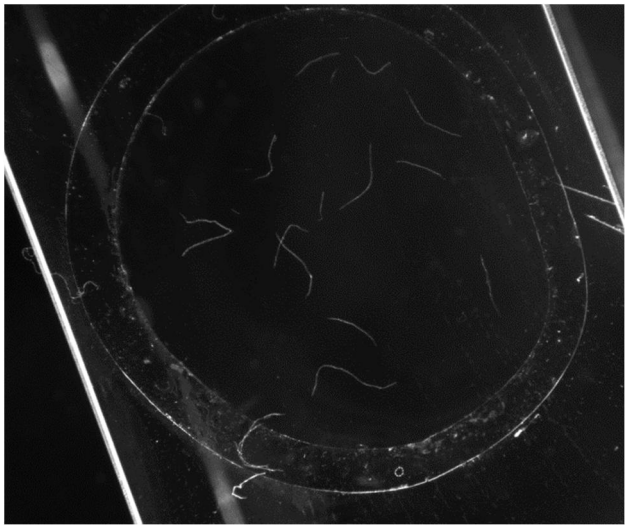

Figure 4.9 Ring light dark field, top camera sample

The results presented in Table 4.1 show relative successes except for a single failure in the second sample. Without this sample, the success rate would be reasonable for such segmenting problem.

Table 4.1 Ringlight results for top camera

	Total fibers	Found fibers	Partials found	Ratio
1	18	7	5	0.67
2	13	3	0	0.23
3	16	10	1	0.69
4	15	10	3	0.87
5	12	11	0	0.92
6	13	9	2	0.85
7	14	9	4	0.93
8	17	12	3	0.88
9	19	11	3	0.74
10	21	16	3	0.90
Total	*158*	*98*	*24*	*0.77*

However, with the side camera view there is a serious problem with the contrast and reflections. Figure 4.10 demonstrates a sample of this situation. The result was that none of the fibers in the resulting images could be recognized. Instead the middle part of the whole image and the ring holding the fibers was falsely threshold as a big white area. This is a result from a reflection on the water surface and low contrast. Because of this problem the ring light cannot be considered as an option for the final design and was disqualified.

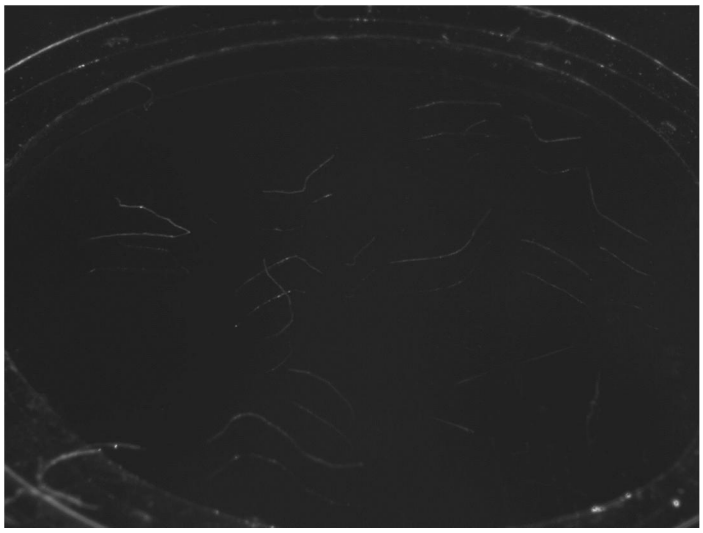

Figure 4.10 Ring light dark field sample from side view camera

4.3.2 LED array dark field

Reaching of successful results with this illumination type was more challenging than the first tests indicated. The positioning of the LED modules and the adjustments of voltage (power) could not improve the contrast adequately. The positioning of the light source was problematic because it might block the microgripper actuator movements. During this test the location of the LED arrays was not realistic. Adding a third similar LED might also have improved the results but would consume more space. Only two arrays were available for test use in this phase of the research.

As Figure 4.11 indicates this illumination strategy performs weakly with the top camera. Even the fibers that are perpendicular to the LED light direction (from left and right to the image) are imaged with a weak contrast. The direction of the fiber clearly has effect on the contrast of the fiber in the final image. This is also a problem for this illumination solution.

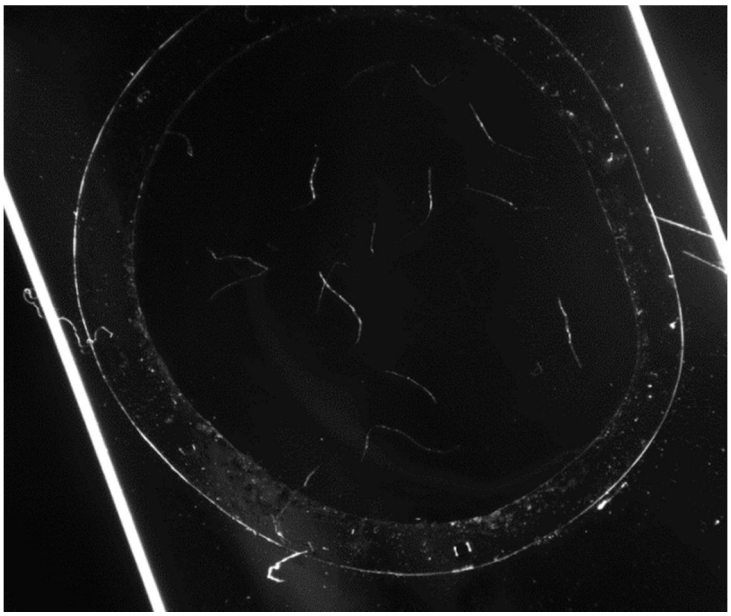

Figure 4.11 LED array dark field illumination test image

Table 4.2 Test results from top camera with the LED array dark field illumination

	Total fibers	Found fibers	Partials found	Ratio
1	14	0	2	0.14
2	11	1	3	0.36
3	15	1	5	0.40
4	16	0	1	0.06
5	13	10	1	0.85
6	12	3	5	0.67
7	14	1	6	0.50
8	17	2	6	0.47
9	23	0	6	0.26
10	25	4	2	0.24
Total	*160*	*22*	*37*	*0.37*

The results in Table 4.2 confirm that there is a problem with the performance of this illumination strategy. The success rate of 37% is inacceptable for the top camera. The reasons for this failure are the lack of illumination power relative to the distance from the subject and the reflections caused by the direction of the light.

The side view camera actually performed better than the top camera. This may be seen also from Image 4.12. Even though reflections of fibers are seen on the glass in the sample images, they did not distract the fiber recognition algorithm. However, both cameras should produce acceptable results simultaneously using the same illumination. This is currently not true with LED array dark field illumination. The calculated results are shown in Table 4.3.

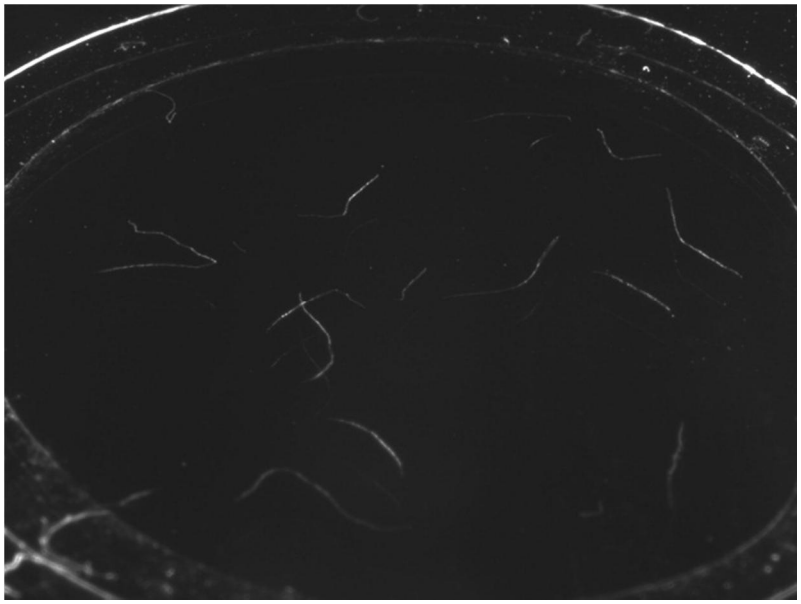

Figure 4.12 Led array dark field sample from side camera

Table 4.3 Test results from side view camera with the LED array dark field illuminatio

	Total fibers	Found fibers	Partials found	Ratio
1	15	9	1	0.67
2	13	6	0	0.46
3	13	8	1	0.69
4	16	7	0	0.44
5	15	9	0	0.60
6	14	7	3	0.71
7	14	6	2	0.57
8	14	6	0	0.43
9	16	6	3	0.56
10	18	10	0	0.56
Total	*148*	*74*	*10*	*0.57*

4.3.3 Polarized backlight illumination

Figure 4.13 shows how polarized illumination gives improved results with the top camera. The test images are superior in quality compared to the earlier test samples. As the Table 4.4 shows, this illumination also produces good numerical results.

Figure 4.13 Top camera sample image of polarized illumination

Table 4.4 The results from top camera

	Total fibers	Found fibers	Partials found	Ratio
1	17	13	3	0.94
2	14	13	1	1.00
3	17	17	0	1.00
4	17	14	2	0.94
5	13	12	0	0.92
6	14	11	2	0.93
7	12	9	2	0.92
8	16	10	3	0.81
9	22	15	2	0.77
10	22	17	2	0.86
Total	*164*	*131*	*17*	*0.90*

Figure 4.14 gives an example how even the challenging side camera view is showing the fibers with a good contrast. The results are shown in Table 4.5.

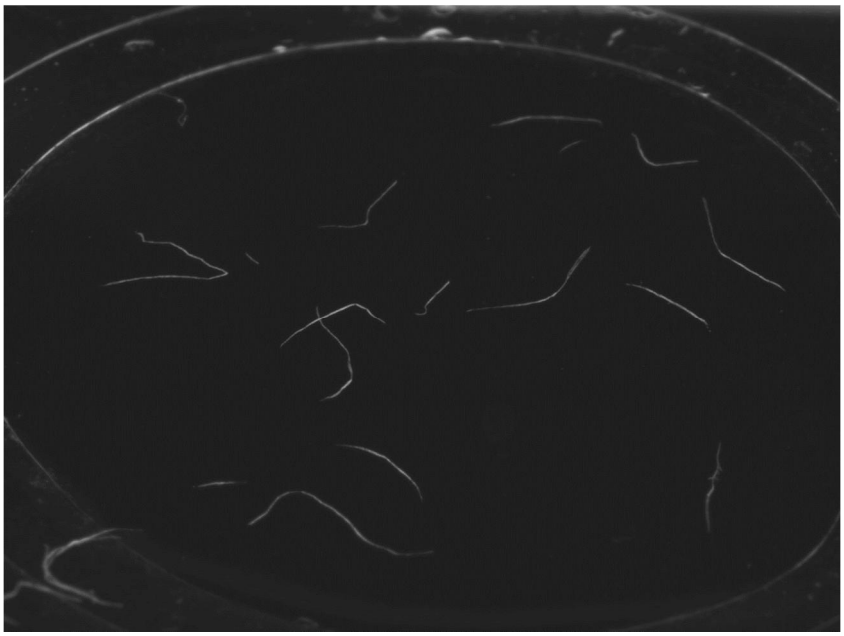

Figure 4.14 Side view from the polarized backlight setup

Table 4.5 Results from the side view of polarized illumination

	Total fibers	Found fibers	Partials found	Ratio
1	18	11	0	0.61
2	14	11	1	0.86
3	16	13	1	0.88
4	20	14	0	0.70
5	14	9	1	0.71
6	16	10	1	0.69
7	15	8	2	0.67
8	20	12	1	0.65
9	22	11	0	0.50
10	24	11	1	0.50
Total	*179*	*110*	*8*	*0.66*

4.4 Prototype design of polarized illumination

After the larger image sets were compared and platform requirements taken into account, the best illumination technique for further development was chosen. Polarized illumination using a backlight and polarization filters on both sides of the fiber sample was selected. A way of integrating this kind of illumination into the platform had to be designed. A prototype was built and tested first, to confirm the principal ideas and solutions designed as an answer to the problem. The components and methods of this prototype are explained in this section.

4.4.1 Prototype construction

The platform has a limited amount of vertical space available for the illumination module. The requirements for the light source included relatively high power, small size vertically and horizontally, but large enough illumination angle to produce a balanced illumination for a transparent sample cup holding the fibers. LED technology was considered especially suitable because of the relatively low warming effect.

High-power LED components fulfil the mentioned requirements conveniently. A 30 W power LED component with a 5x6 matrix of 30 surface mounted LEDs was selected as the light source. Part of the bottom metal plate of this component was cut away to minimize the diameter of the light source down to 42 mm.

The LED is of a common high power type and no manufacturer was mentioned as it was purchased on eBay online auction. Similar chips are manufactured by several companies, for example Epistar. The specifications of this light source include a viewing angle of 120 degrees, which suits the needs of the system under design.

The polarized backlight illumination needs one polarizer between the light source and the subject. With the chosen LED light source also diffuse filtering is needed to even up the produced illumination. A square piece of 2 mm thick diffusing plastic is set directly on top of the LED surface and part of diffusing filter used originally in an LCD monitor is set 1 cm above the previous filter. Together these two diffusers produce even illumination and blur the matrix structure of the light source, which would otherwise be visible in the resulting image. A hollow cylinder is used in abducting of the second diffuser from the parts below. Together these two diffusers produce a suitable pattern and balanced illumination for the whole area inspected.

The lower polarizer is set directly on top of the second diffuser. The desired polarization effect is only achieved when a second filter is installed between the sample subject and the camera. At this prototype phase a laboratory arm was used to hold the second polarizer, which was rotated until direct light from the LED was blocked. The side camera also needs a polarizer in front of it, so a linear polarizer photography filter is attached to the front of the lens system. This is a Kood polarizer filter with a 52 mm thread. Figure 4.10 shows the LED (D) component at bottom right, diffusing filters (A, C) on left and a part of polarizer sheet (Edmun Optics product # 38493) (B) on top right.

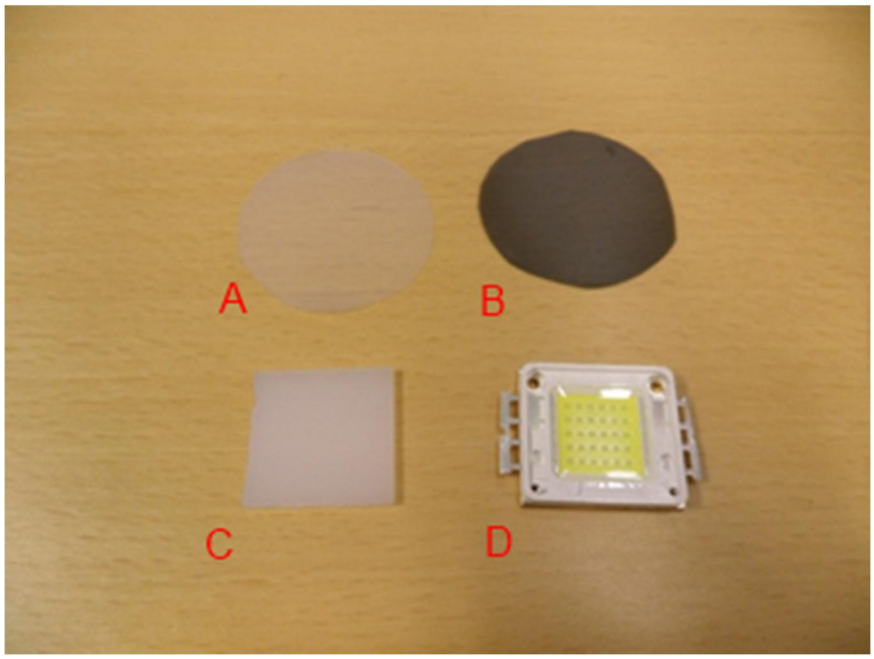

Figure 4.9 Illumination components for the prototype and final version of polarized illumination: top diffuse filter (A), polarizer (B), lower diffuser (C), LED light source (D).

The architecture at this phase is very simple and tries only to simulate the later version discussed in the next chapter. Figure 4.10 is showing the construction with labels. The LED (2, D) is located on top of aluminium cooling plate (1). The cooler was later discarded because of the space it consumes and the fact that the LED does not warm up detrimentally in this kind of use. The cylinder holder (3) is made of brown matte cardboard. It is taken from a regular tape roll and has a height of 15 mm. It is holding the diffuser (4, A) and the polarization filter (5, B) directly on top of it. The fiber sample pool is directly above the filters in this case. An extra diffuser (C) of 1 mm thick plastic is located on top of the LED light to blur the matrix form of the LED source from the images. The structure is shown as a simplified scheme in Figure 4.11. Both of the platform cameras were also using a polarization filter in front of them to create the desired illumination effect.

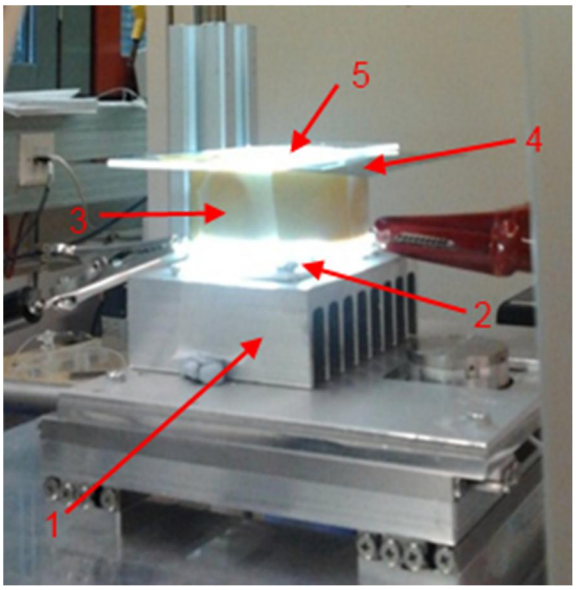

Figure 4.10 Polarized illumination prototype setup: 1. cooling plate,
2. LED illumination, 3. cylinder holder for the filters, 4. polarizer, 5. diffuse filter

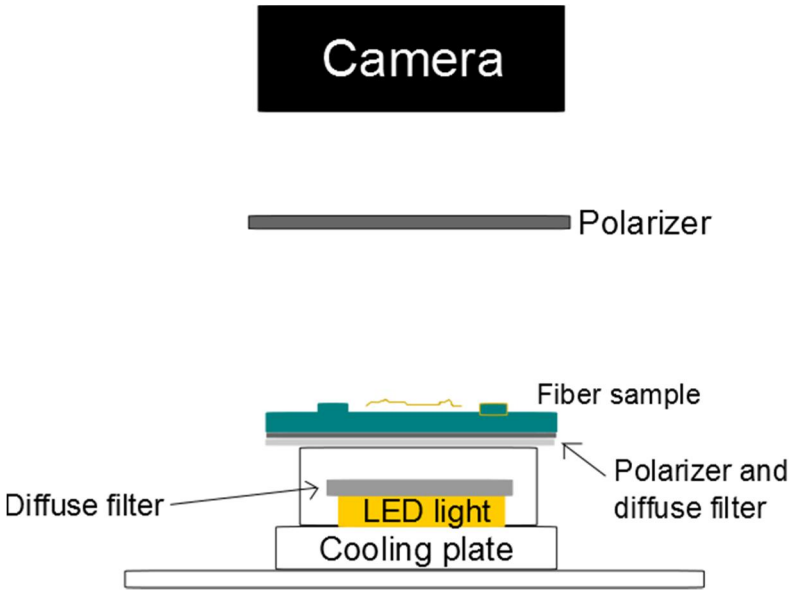

Figure 4.11 A scheme of the prototype structure

4.4.2 Prototype results

The results with the prototyping phase of the illumination module are shown in Table 4.6 and Table 4.7 and discussed below. There was a file corruption error with the tenth sample of the top camera results, which caused that row to be empty. A rate of 92% success is 2% higher than the rate of polarized illumination in the first tests. The results from the side view gave more than 10% improvement from the earlier test. For the first time during this thesis also the side camera result was good enough to consider it a success. The results are calculated as explained in Section 4.3.

Table 4.6 Results for the polarized illumination prototype from top camera

	Total fibers	Found fibers	Partials found	Ratio
1	17	16	1	1.00
2	25	25	0	1.00
3	14	11	0	0.79
4	21	18	0	0.86
5	19	15	1	0.84
6	22	21	0	0.95
7	22	19	0	0.86
8	18	17	1	1.00
9	19	16	2	0.95
10	-	-	-	--
Total	*177*	*158*	*5*	*0.92*

Table 4.7 Side view results of the polarized illumination prototype

	Total fibers	Found fibers	Partials found	Ratio
1	21	17	4	1.00
2	20	19	1	1.00
3	27	18	4	0.81
4	12	6	1	0.58
5	18	12	1	0.72
6	12	10	0	0.83
7	14	9	1	0.71
8	17	13	0	0.76
9	15	8	1	0.60
10	19	11	0	0.58
Total	*175*	*123*	*13*	*0.78*

Evaluating this prototype confirmed that the use of polarized backlight illumination would be a suitable choice. In practice it has some challenges related to the mechanical design. This causes the need of new structures into the platform to maintain the functionality of the actuators with such new illumination structure.

4.5 Conclusions

After evaluating different options, the polarized illumination technique qualified as the most suitable one. The ring light dark field illumination was discarded because of the side camera problems, LED array dark field because of weak overall performance. The side view images of the ring light solution produced defect images by the image processing algorithm and resulted in zero recognized fibers. Both of these solutions would have been problematic also in terms of the space usage of the light sources. The ratio of successfully recognized fibers compared to the total fibers in the images is shown in Table 4.6.

Table 4.6 Fiber recognition success of different illumination solutions

	Top camera	Side camera
Ring light	77%	0%
LED arrays	37%	57%
Polarized illumination	90%	66%

Even though the polarized illumination and the need of backlighting cause some challenges to be implemented into the platform, it is considered to be the best option because of the superior performance. It is also after all easier to build inside the existing mechanical and robotic structure compared to LED array lighting. Those large arrays would block the actuator movements. Also ring light illumination has some problems with the shadows caused by the actuators.

A rough prototype demonstrating the structure of the new illumination module was tested to confirm the functionality of the solution. This system explained in Section 4.4 gave 92% ratio for the top camera and 78% for side view. After the successful results, the design of the new polarized illumination module was continued.

5 DESIGN OF THE ILLUMINATION MODULE

The selected illumination method could not be implemented into the current state of the platform directly. The lower level of the platform architecture carrying the XY-table and the rotary table needed to be modified in order to allow the polarized backlight illumination for the fibers. The important functions such as the movements of the sample pool and actuators had to be preserved. These requirements and the resulting illumination structure for the new module are described. The module is also verified and the results discussed in this chapter.

5.1 Requirements

Maintaining the platform structure as previously was preferred during the illumination design of this thesis. This caused limitations for the size of the new module. It must fit the given space and leave space for the actuator movements. Also the locations of the fiber sample pool were preferred to be approximately the same. The requirements of the illumination module are defined in this section.

The space allocation requirements of the new module were simplified. It had to fit inside the current platform space simultaneously leaving space for the XY-movements of the working plane. The new module would need more space in Z-direction between the platform floor and roof. It would be designed maintaining the highest point of the system on the same level as the previous rotary table system had. This allows the other actuators to keep their full movements as previously. Such design was straightforward because the architecture of the platform allowed the simple lowering of the platform floor, which holds the rest of the system related to the XY and rotary movements of the samples.

With the previous setup the platform floor is located 92 mm above the laboratory table plane that the system stands on. This is also the maximum height of the new illumination module. Other restrictions in space allocation exist in the XY-oriented space on top of the platform floor. The floor is 175mm x 175 mm in area. This includes the area used by the support pillars in each corner of the plane, which restrict the movement of the XY working plane also.

The fundamental requirement of the new illumination system and construction was to create a new rotary table system that would allow backlighting. Simultaneously, rotation of the fibers without rotating the lower polarization filter is required. Synchronized rotation of two filters would be too complex and problematic. The whole module would be moved by linear SmarAct SLC-1780 positioners and the fibers rotated with an SR-

1908 rotary table. The working plane of the new design also needs suitable screw holes for attaching of a FemtoTools FT-S micro force sensor on top of it.

5.2 Construction solutions

This section addresses the construction solutions designed for the new illumination module. Both mechanical and optical solutions are described.

5.2.1 Mechanical solutions

The main challenge of the structure was the rotation of the fibers without rotating the polarizing filter in front of the LED light. Most of the platform could be maintained as it was but parts on top of the XY-table needed changes. Also, some new components needed to be added to the system. The behaviour of the actuators would stay the same but the illumination and the architecture of the working plane would change.

To replace the current XY-table support plane and the rotary table sample pool, a new three-layer XY-construction was designed to be installed on top of the XY-table actuator. This design includes the same rotary table actuator as earlier but it is equipped with different attachments. The aluminium fiber cup on top of the rotary table was removed and instead a hollow cylinder (5) was attached to the rotating part of the table. The cylinder would hold a disc with a circle hole on top of it, named as the rotary lid (8). This hole is designed to hold a transparent glass disc serving as the sample pool.

The hole in the rotary table structure was used to bring a hollow wire pole (4) through it to support a round support disc (6), which would carry the actual illumination source. The electricity is brought to the LED source through the hollow pole. The lower, static polarization filter and the diffusers would also be located on this plane. This architecture would be able to keep the illumination and the filters static while rotating the surrounding cylinder.

Two bottom plane (1) and the rotary plane (3) of this new module serve as support. The bottom plane holds four support pillars (2) in each corner supporting the rotary plane, which holds the rotary table and the working plane (7), which attaches the system to the XY-actuators. The wire pole (4) supporting the illumination is attached to the bottom plane with an M4 screw through the bottom. The working plane has screw holes for attaching of the micro force sensor.

The rotary plane is held on the correct height by 4 M4 screws from the sides, attached through the holes in the support pillars. The correct height of this plane is 23 mm from the bottom of the module. The plane has an embedding for the rotary table, which is 3 mm deep. The drawings of these parts are presented in Appendix A of this thesis in more detail. The components of the new module are shown and numbered in Figure 5.1. These parts were manufactured at Jonelec Oy, a company in Kangasala, Finland. Figure 5.2 shows the module completely installed to the platform.

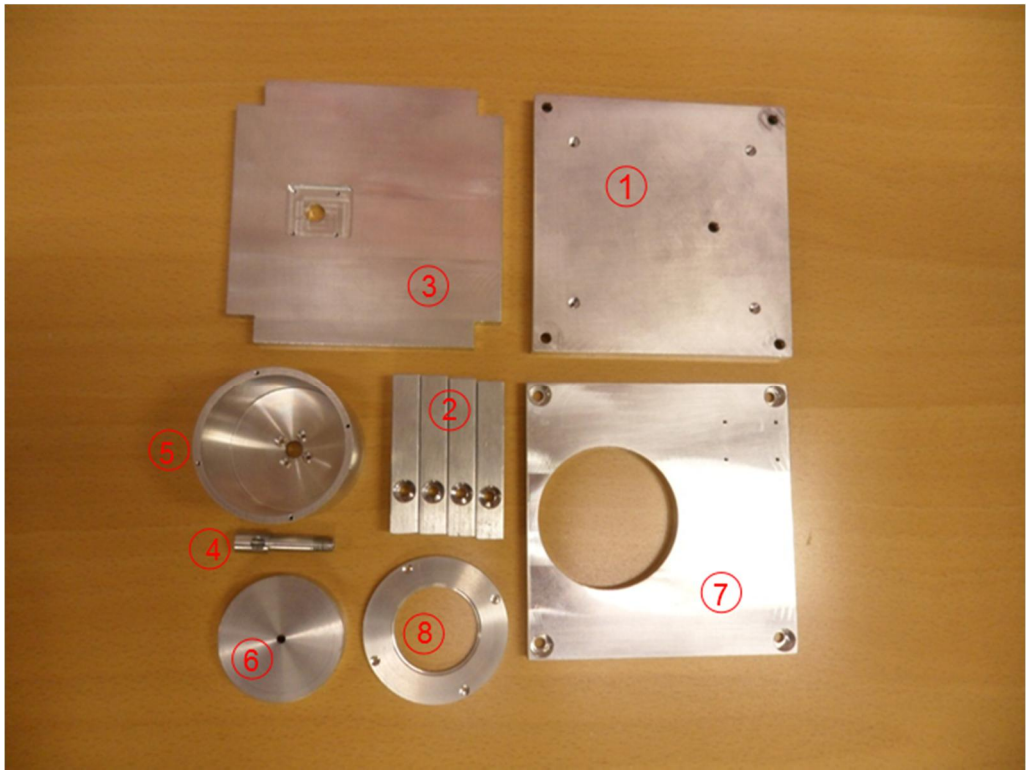

Figure 5.1 The new construction parts for the illumination module: Bottom plane (1), support pillars (2), rotary plane (3), wire pole (4), cylinder (5), support disc (6), working plane (7) and rotary lid (8).

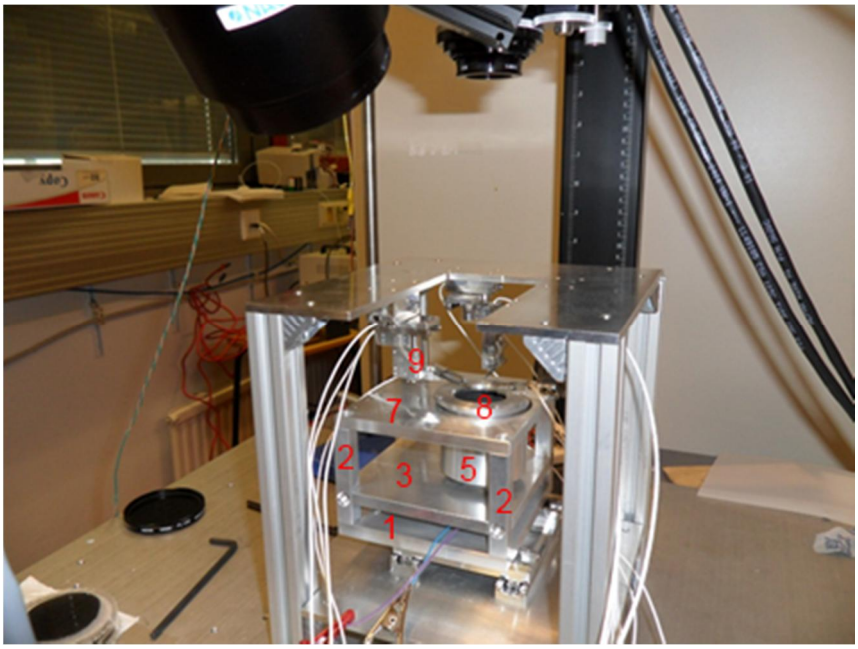

Figure 5.2 New illumination module installed to the platform: Bottom plane (1), support pillars (2), rotary plane (3), cylinder (5), working plane (7), rotary lid (8). Parts (4) and (6) are located inside part (5), thus not visible in this image.

The dimensions of this module are 100x100 mm^2 in area in XY plane. This leaves space for the XY-actuators to shift the module left and right. The height of the system from bottom of the base plane to the surface of the working plane is 72 mm. The highest part of the rotary lid is 4.5 mm above this level making the total height 76.5 mm. This is less than the distance, which the bottom of the original platform can be lowered. Thus, it fulfils the requirements of maximum height of the new module. Now the module may be directly attached to the XY actuators and implemented to the platform as in image 5.3.

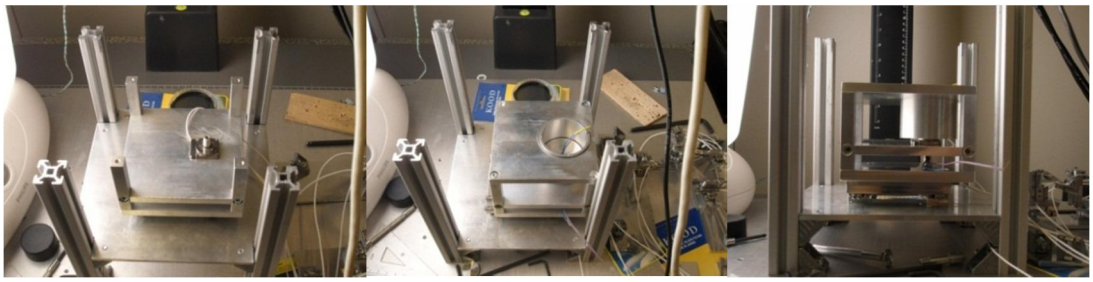

Figure 5.3 Installing of the new illumination module to the platform

5.2.2 Optical solutions

With the previous design of the working plane and rotary table, the cup of the rotary table holding the fiber sample, was made of non-transparent aluminium metal. Polarized illumination would need the use of backlight illumination. The sample pool would need to be transparent as in the illumination research of this thesis. A similar solution as explained earlier in Section 3.1.4 is selected. A round piece of glass, equipped with a ring shaped boundary to hold the sample solution is embedded on the top of the rotating cylinder part.

Polarized light in this design also required the use of two polarization filters: one in front of the illumination source and another in front of the camera lens. The target fibers would be located in between these filters. The fibers needed to be rotated in order to have their endpoints available for the grippers in correct directions. The two polarization filters must be set perpendicular to each other in rotating direction to achieve the desired illumination effect. Figure 5.3 illustrates the construction of the illumination related components of the new module.

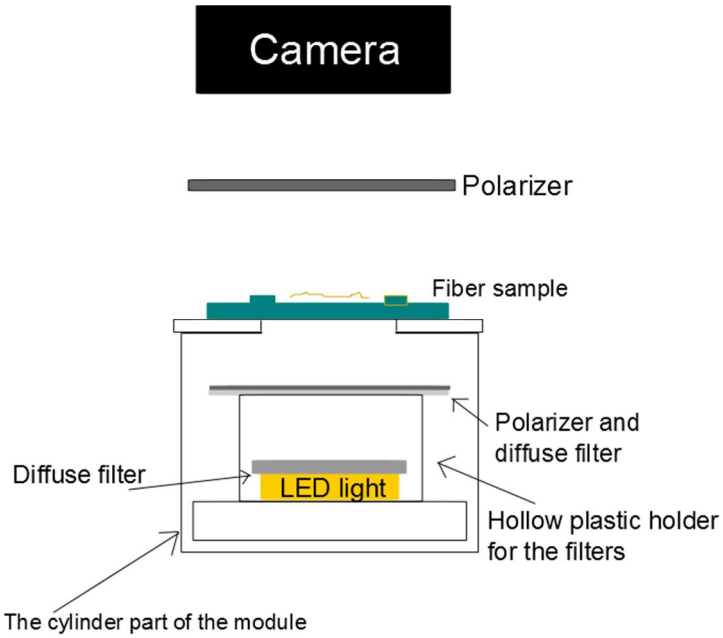

Figure 5.4 Illumination configuration of the designed module

The selected illumination source and filters were the same as described in Section 4.3.1.

The inside of the rotating cylinder part was sealed with a layer of black cardboard in order to minimize the reflections hitting the side camera view. The cardboard pictured in Figure 5.4 on the inside face of the cylinder, had a matte surface and black colour to reduce these reflections. A hollow tube was used to hold the filters and only let filtered light out of the tube.

Figure 5.5 Rotating cylinder part with the black cardboard wallpaper

5.3 Verification of the illumination module

Due to the nature of these tests, quantitative analysis of illumination performance was quite difficult. It was challenging to measure the illumination quality with numerical indicators. The most important test method in this thesis was counting the amount of correctly threshold and recognized fibers as a ratio out of the total number of individual fibers inside the imaged area. This is a very practical approach for the quality measurement. Basically it means using the same methods in recognizing the fibers as would be used when the platform was in real use. More theoretical and mathematical indices do exist, but those were left out as too complicated for this thesis and are not necessarily the best indices with a problem of this kind. The results are calculated similarly to the earlier results as described in Section 4.3.

5.3.1 Methods and setup

The final illumination solutions are tested and evaluated basically the same way as when the different illumination techniques. The new mechanical parts were installed to the existing platform and the lower level of the platform was lowered almost to the bottom plate level. This set the level of the sample cup to the same height as it was with the previous structure for other illumination systems. Sample set of ten images were taken and analysed. Each image shows a view of the transparent glass slide supporting random amount of fibers.

Both cameras were set up and zoomed so that the circle formed by the edge of the fiber cup filled most of the image area. The exposure and aperture settings for each camera were optimized visually and by hand because of the complexity of the system any mathematical optimum would be very difficult to calculate exactly. The resulting image from each camera was aimed to have a good contrast with a dark background without changing the settings during the change of fiber samples. Also the power used by the LED light was chosen close to the maximum and visually optimized by the user to produce a suitably powerful illumination for both cameras. Too much power would distract the side view camera causing reflections from the edges of the system to hit the optics.

5.3.2 Results

The final results of the new illumination system are shown in this section. Figure 6.2 shows an example of the performance of the designed illumination system. The fiber count results are shown in Tables 6.1 and 6.2.

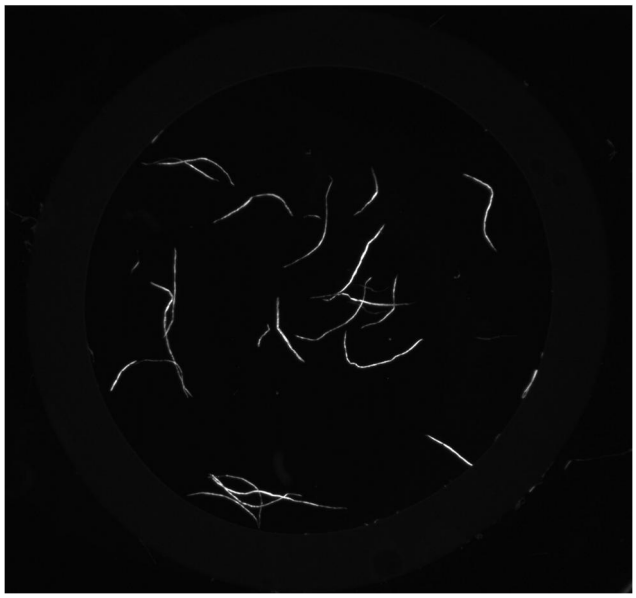

Figure 5.2 Top camera view with final illumination design

Table 6.1 Top camera results calculated with final design of polarized illumination

	Total fibers	Found fibers	Partials found	Ratio
1	10	5	2	0.70
2	14	10	2	0.86
3	15	11	2	0.87
4	9	6	2	0.89
5	15	12	2	0.93
6	19	16	2	0.95
7	13	6	3	0.69
8	20	14	2	0.80
9	13	10	2	0.92
10	16	12	3	0.94
Total	*144*	*102*	*22*	*0.86*

The total average success rate of correctly recognized fibers out of total individual fibers in the 10 images is as high as 86%. Some of the sample images had a lower rate but variance is normal in this kind of problem. The fibers are thin, curled and twisted around their axis, which challenges observing them accurately with the vision system in question. Sometimes the light does not hit the fiber surface in a straight angle but rather sideways. This will make the fibers in these polarized illumination images darker and melt into the background of the image, which is also dark or black. The fibers also have various proportions especially in thickness and are sometimes seen in the original image dark. Those fibers may not be segmented into the correct class by the software.

As Figure 6.3 and Table 6.2 show, the side camera results are still weaker than the ones from the top camera. This cannot be avoided without compromising much of the top camera results. The side camera position causes the polarizing effect of the complete system to be only partial. This is a result of internal reflections of the system and the loss of illumination travelling from the LED light. In this case the side camera and the optics it uses have a better ability in capturing light generally than the camera system on the top of the platform. This makes the images visually show better lit but is indeed a result of the light capturing ability

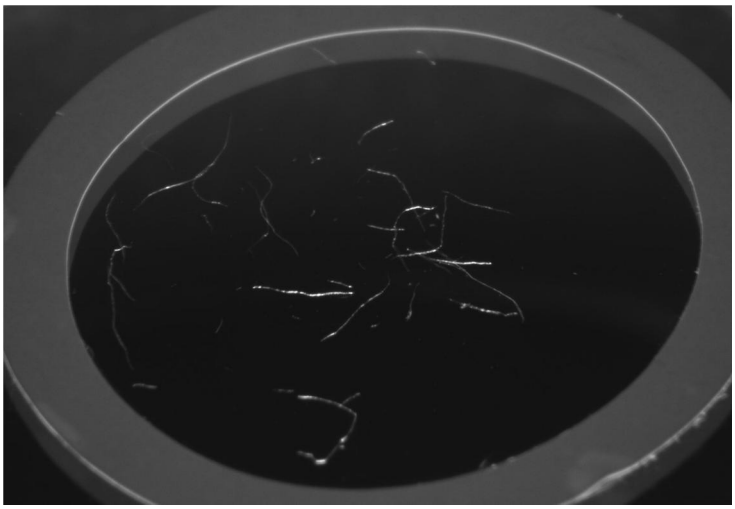

Figure 5.3 Side camera view with final illumination design

Table 6.2 Side camera results

	Total fibers	Found fibers	Partials found	Ratio
1	8	5	2	0.89
2	12	7	3	0.83
3	13	8	1	0.69
4	8	3	2	0.63
5	13	10	2	0.92
6	14	11	1	0.86
7	9	5	1	0.67
8	15	10	2	0.80
9	8	5	0	0.63
10	13	4	4	0.62
Total	*113*	*68*	*18*	*0.76*

The results with the new structure and illumination are even better than with the prototype version, even though some compromises had to been done during the design. Other improvements in the design seem to have compensated for those compromises.

5.3.3 Summary

The design shows a good performance and the improvement from the earlier illumination is remarkable. With this illumination solution, 86% of the fibers were correctly recognized from the top camera and 76% from the side camera. During the whole thesis work the overall performance has improved even though the top view ratio is less than given in the prototype tests (92%). Visually the images have a strong contrast between the fibers and the background. This is a significant improvement from the previous illumination system described in Section 3.1.3 and in Figure 3.3.

6 CONCLUSIONS AND FUTURE WORK

The conclusions and future work of this thesis work are presented in this chapter.

6.1 Conclusions

The illumination design and research performed in this thesis improves the illumination of a microrobotic fiber platform. The platform finds paper fibers from the sample images with a software previously designed. Microactuators are used to place the fibers and manipulate them. These actuators are run according to the images produced with two cameras. Illumination of this platform was poor for this kind of machine vision system and was therefore researched further.

In the beginning of the thesis work, different illumination strategies were experimented and the weakest ones discarded. Out of the functional solutions, three best were compared with each other using a very basic architecture with each of them. These solutions were dark field illuminations using ring light or LED arrays and a polarized backlight illumination system. Using the fiber recognition algorithm designed for the platform applications, the rate of successfully found fibers was calculated for each image.

The total ratio of found fibers out of total fibers in the images was used as the numerical value to describe the image quality with each illumination. Results were calculated for two cameras, top and side view, with each illumination. The calculation resulted in ratios described in table 6.1. The ratios were calculated as described in Section 4.3, where also more accurate calculations are shown.

Table 6.1 Summary of the results from Section 4.3

	Top camera ratio	Side camera ratio
LED array dark field	0.77	0
Ring light dark field	0.37	0.57
Polarized backlight	0.90	0.66

As the results propose, polarized backlight was selected for further research. A simple prototype was built first to confirm the convenience of the principal ideas of the final polarized illumination module. The prototype was tested in similar manner and resulted in ratios of *0.92* for top camera and *0.72* for the side view camera.

The success of the prototype confirmed the continuation of the final module design for a polarized backlight system to be implemented to the fiber platform. The challenges resulting from the platform space limitation were solved and the structure requirements for the new module fulfilled as discussed in Chapter 5.

The ratio of the top view with the final structure is *0.86*, which is lower than the prototype yield. The overall image quality and the improvements with the side view however compensate for this fault. The success ratio with the side camera view is *0.76* and is the highest performance from this camera. The side view was problematic because the camera views the sample in an angle of about 45 degrees, thus light is not traveling directly.

Judging by these results, polarized light with the design presented in this thesis is a feasible solution. Optimization of the illumination might still be possible, but the new illumination is already far superior to the original coaxial illumination of the platform. The summary of the results from each phase in the design of the final solution are given in Table 6.2.

Table 6.2 Summary of the results during the research on polarized illumination

	Top camera ratio	Side camera ratio
Polarized illumination test	0.90	0.66
Prototype	0.92	0.72
Final result	0.86	0.76

In this problem, the objective is to find the fiber endpoints to be able to grasp them with micro grippers. The actual automated grasping was still under research during this thesis, but the aim of improving the illumination was reached in this thesis.

6.2 Future work

To continue the work of this thesis and the projects related, following aspects may be considered.

6.2.1 Illumination improvements for the platform

There were details with the illumination of the platform, emerging during this thesis work left out of current research. Practically the most important aspect is the platform general illumination. This means the illumination of the actuators, which also have to be visible by the camera in order to grasp the fibers with them. This was researched insufficiently in this thesis. Images including these micro gripper jaws and chess board target sheets were taken but these targets demand different illumination. A solution for this problem was already tested in other research during this thesis but was not discussed here.

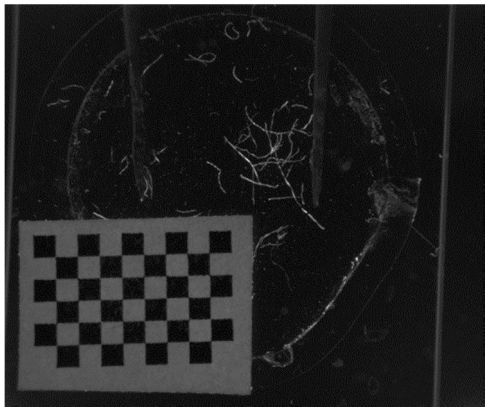

Figure 6.1 Example of polarized illumination showing
the illumination with other targets than the fibers

The camera setup and image processing software were also under research simultaneously. Possible changes in the imaging hardware of the system might cause the need of adjustments on the illumination and polarization filtering preferences. For example, it is decided that the current top view camera will be replaced with a similar as the side view camera was during this thesis. Such modification may need adjustments in the diffuse filter strength because of the different optical qualities of the system. The Navitar Zoom 7000 lens has different aperture and focal length preferences, which might change the view slightly. However, the principle of the new illumination module architecture is feasible with any camera system.

With the help of image processing, the performance of fiber recognition could be further improved. Optimizing the fiber contrast by image processing algorithms, the segmenting software would have even better performance. Of course the aspect of computational simplification still needs to be taken into account.

6.2.2 Fiber bond imaging

Measuring the fiber bond strength with a micro force sensor would be more accurate with the ability to estimate the bonded area of the two fibers. This should happen visually or otherwise, without breaking of the bond. Polarized illumination may be utilized for such estimation. When the polarizers are set in different angle than for the normal fiber imaging, they are emphasizing the bonded area instead of the whole fiber. The bonded area turns dark in the image while the fibers remain light.

A research exists stating that the results obtained from an image of the bond are not confident as such from polarized illumination. The assumed bonded area can be seen in the images without other manipulations but in this research it is shown that only 63% of the bond area measurements were confident when compared to a cross-section of the bond area. However, by dying another one of the bonded fibers it is possible to improve the results. With such procedure, they could be used to quite accurately estimate the bonded area between the fibers. [27, 28, 29]

REFERENCES

[1] H. Matsuoka, T. Komazakia, Y. Mukaia, M. Shibusawaa, H. Akanea, A. Chakic, N. Uetakec and M- Saitoa, ”High throughput Easy Microinjection with a Single-Cell Manipulation Supporting Robot”, *Journal of Biotechnology,* Vol. 116, No.2, 2005, pp 185-194.

[2] C. I. Haider, T. Althaus, G. Niederreiter, M. J. Hounslow, S. Palzer and A. D. Salman, 2012. “A micromanipulation particle tester for agglomeration contact mechanism studies in a controlled environment”, *IOP Publishing Measurement cience and Technology.* Issue 23, 2012, No. 105904. 12p.

[3] Stratton, R.A. 1991. “Characterization of Fiber-fiber Bond Strength from Paper Mechanical Properties”. International Paper Physics Conference, Kona, Hawaii 1991. Institute of Paper Science and Technology, Atlanta, Georgia. IPST Technical Paper series, number 381.

[4] Axelsson, A. 2009. “Fibre based models for predicting tensile strength of paper”. Master of Science Thesis, Luleå University of Technology. Department of Skellefteå Campus, Wood Engineering and Technology Division. 36p.

[5] Saketi, P. & Kallio P. 2011. ”Microrobotic Platform for Making, Manipulating and Breaking Individual Paper Fiber Bonds”, IEEE International Symposium on Assembly and Manufacturing (ISAM)

[6] Saketi, P., 2010. “Microrobotics Platform for Manipulation and Flexibility Measurement of Individual Paper Fibers”. Master of Science Thesis, Tampere University of Technology, Department of Automation Science and Engineering. 94p.

[7] Types of reflection http://www.sciencelearn.org.nz/Contexts/Light-and-Sight/Sci-Media/Images/Types-of-reflection 13.08.2012

[8] Thin lens formula http://physics20p1.blogspot.fi/2011/12/thin-lens-equation.html

[9] Hecht, E. Optics. 4th edition. San Francisco. Pearson Addison Wesley 2002. ISBN: 0-321-18878-0. 698p.

[10] Linear polarization filter http://en.wikipedia.org/wiki/File:Wire-grid-polarizer.svg

[11] Tech Note TN-702-2. Document Number: 11212, 2011. Introduction to Stress Analysis by the PhotoStress® Method. Wendell, NC 27591 USA, Vishay Precision Group, Micro-Measurements. 13p.

[12] Jain, Kasturi & Schunck. Machine Vision. McGraw-Hill 1995. ISBN: 0-07-113407-7.

[13] Gonzales, R. C. & Woods, R. E. Digital Image Processing. 2nd edition. New Jersey. Prentice Hall 2002. ISBN: 0-201-18075-8.

[14] Otsu, N., "A Threshold Selection Method from Gray-Level Histograms," IEEE Transactions on Systems, Man, and Cybernetics, Vol. 9, No. 1, 1979, s. 62-66.

[15] Ander, P., Bauer, W., Heinemann, S., Kallio, P. Passas, R., Treimanis, A., 2011. The Final Report of COST Action E54, “Characterisation of the fine structure and properties of papermaking fibres using new technologies”. Swedish University of Agricultural Sciences 2011; ISBN: 978-91-576-9007-4

[16] Koshel, R. J., 2003. "Optimization of illumination systems," in *Frontiers in Optics*, OSA Technical Digest (CD) (Optical Society of America, 2003), paper TuW3.

[17] Tutorial: A Practical Guide to Machine Vision Lighting - Parts I&II, 2008. National Instruments

[18] Müller, V., “Elimination of Specular Surface-Reflectance Using Polarized and Unpolarized Light”. ECCV '96 Proceedings of the 4th European Conference on Computer Vision - Volume II, pp. 625 - 635

[19] Xiaoyan D., Xiaojuan Y. ; Jinsheng F. ; Chun L. ; Lei W., 2010. ”Surface Defects Inspection System Based on Machine Vision”. IEEE, Electrical and Control Engineering (ICECE), 2010 International Conference. Pp 2205-2208.

[20] Okabe, T.,Akaiwa, M., Shirakawa, T., Yokouchi, T., Sugimoto, T.; 1993. Final Visual Inspection for LSI packages. Industrial Electronics, Control, and Instrumentation, Proceedings of the IECON '93., International Conference, 1993. Vol. 3, pp. 1877-1881

[21] Liu, Y., Kong, L., Wang, X., Jiang, F., 2010. “Research on Image acquisition of Automatic Surface Vision Inspection Systems for steel sheet”. 3rd International Conference on Advanced Computer Theory and Engineering(ICACTE). Vol 6. Pp. V6-189 - V6-192.

[22] Rajarshi, R., 1989. “Automated Inspection of Solder Bumps Using Visual Signa- of Specular Image-Highlights”. Computer Vision and Pattern Recognition. Proceedings CVPR '89., IEEE Computer Society Conference 1989. Pp. 588-596.

[23] Delly, J. G., 2008. “Selected Topics From the Essentials of Polarized Light Microscopy”. College of Microscopy, Westmont, Illinois

[24] Hirvonen, J., Saketi, P., Kallio, P. 2011. ”Automatic image-based detection of paper fiber ends”. Proceedings of SPIE - The International Society for Optical Engineering. Volume 8009, Article number 80092N. 3rd International Conference on Digital Image Processing, ICDIP 2011. Chengdu. Code85726

[25] Heiskanen, V., 2008. “Machine Vision Based Measurement Methods for Flow Characterization in Microfluidic Channels”. Master of Science Thesis, Tampere University of Technology, Department of Automation Science and Engineering. 90p.

[26] Prusi, T., 2012. Private discussion on 9th of November, 2012 with Timo Prusi from the Department of Production Engineering, TUT.

[27] Kappel, L., Hirn, U., Bauer, W., Schennach, R., 2010. “A novel method for the determination of bonded area of individual fiber-fiber bonds”. Nordic Pulp and Paper Research Journal Vol 24 no. 2/2009

[28] Kappel, L., Hirn, U., Gill, E., Bauer, W., Schennach, R., 2010. “Revisiting polarized light microscopy for fiber-fiber bond area measurement - Part I: Theoretical fundamentals”. Pp 65-70

[29] Kappel, L., Hirn, U., Gill, E., Bauer, W., Schennach, R., 2010. “Revisiting polarized light microscopy for fiber-fiber bond area measurement - Part II: Proving the applicability”. Nordic Pulp and Paper Research Journal Vol 25 no. 1/2010. Pp 71-75

7 A. APPENDIX A – ILLUMINATION MODULE DRAWINGS

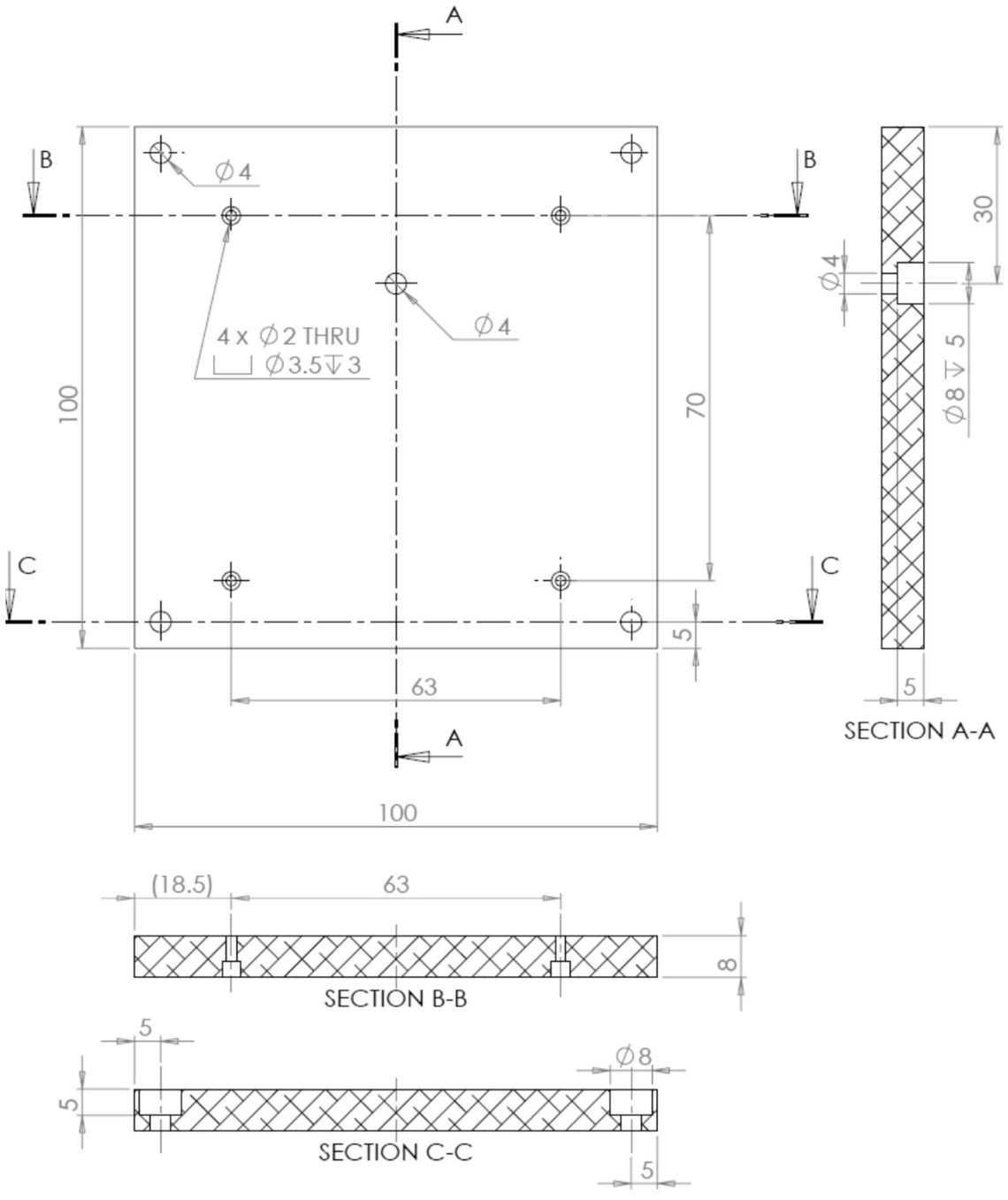

Figure 7.1.1 The bottom plate of the illumination module

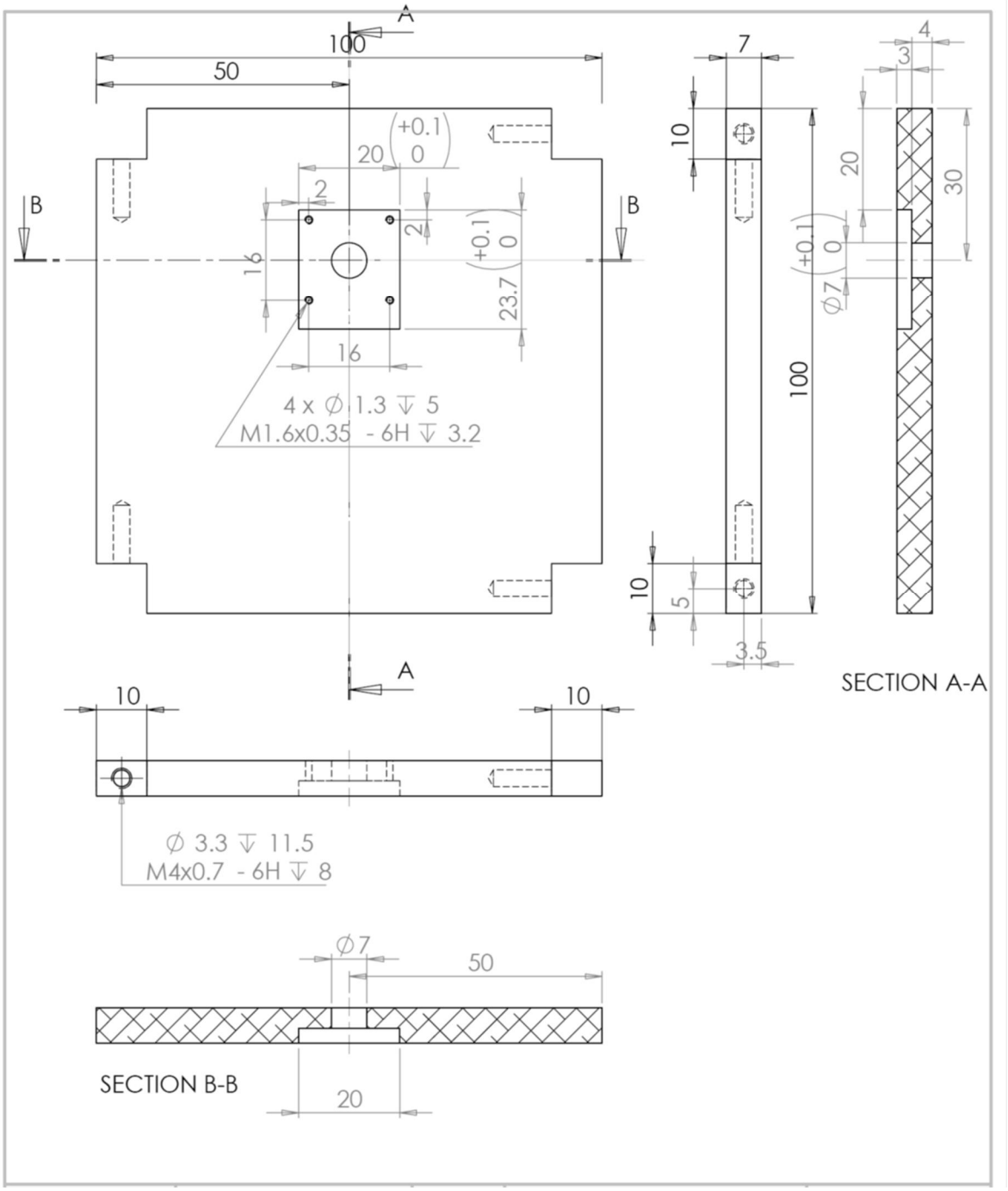

Figure A.2 The middle plate of the illumination module

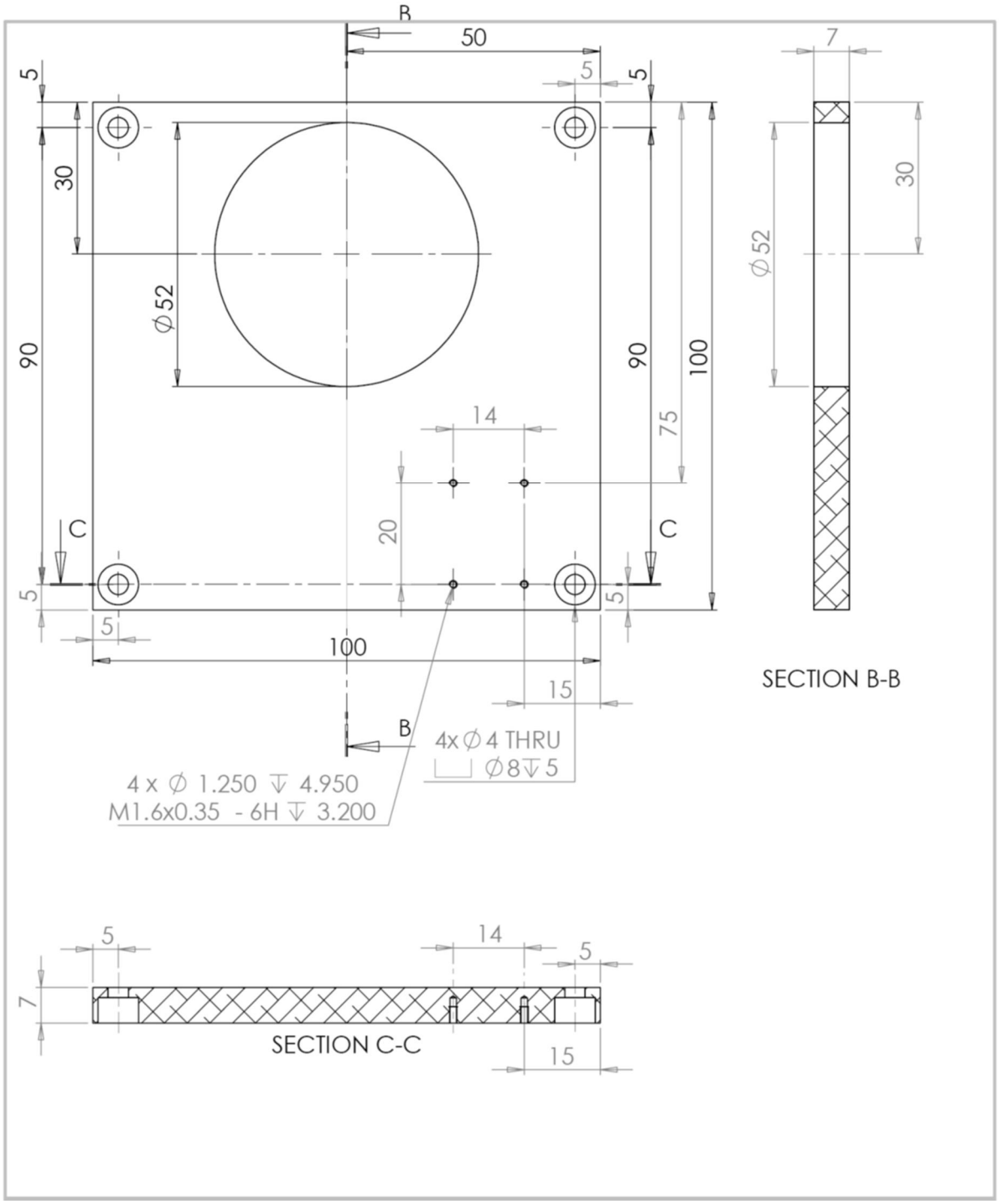

Figure A.3 Top plate of the illumination module

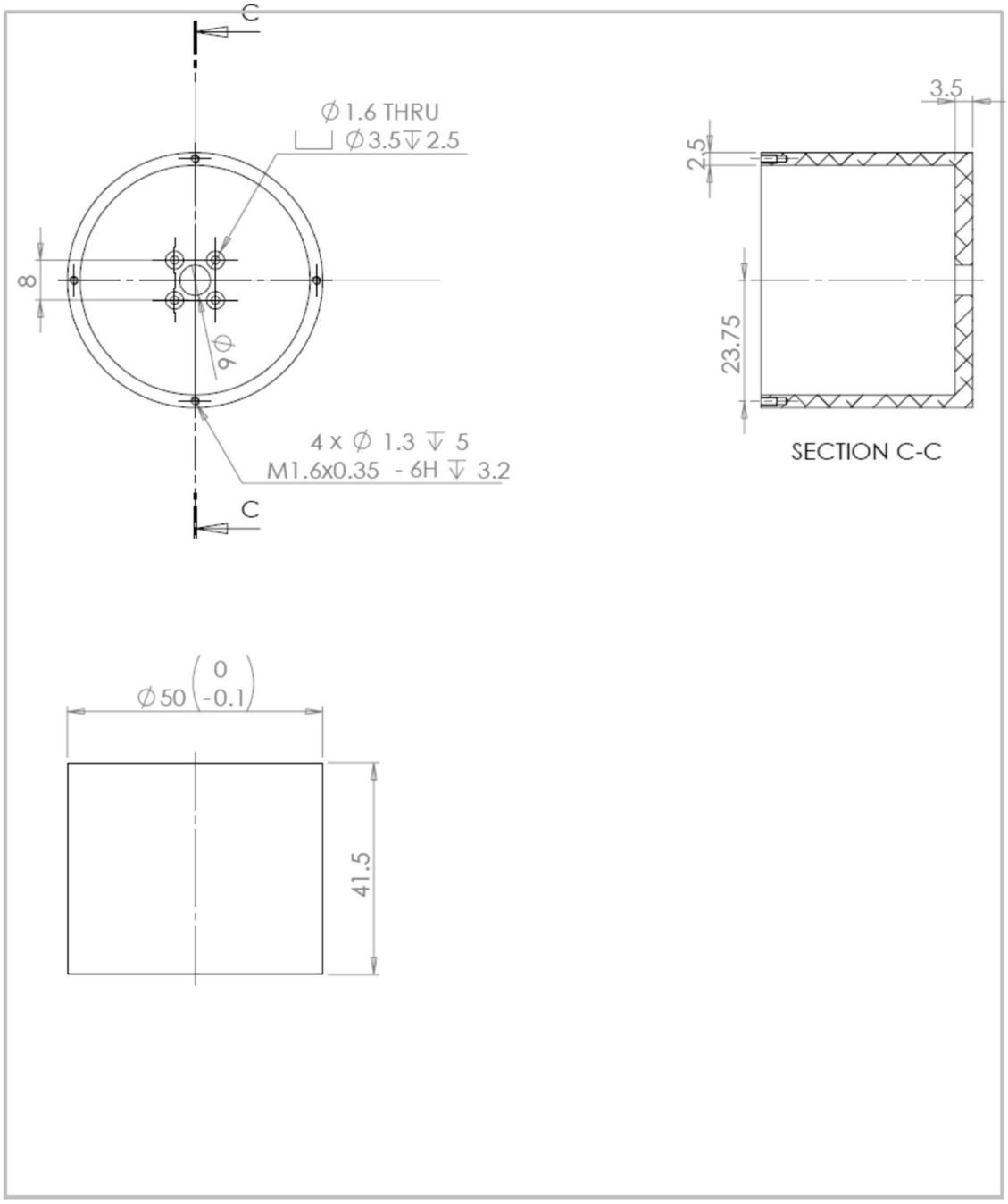

Figure A.4 Rotating cylinder component of the module

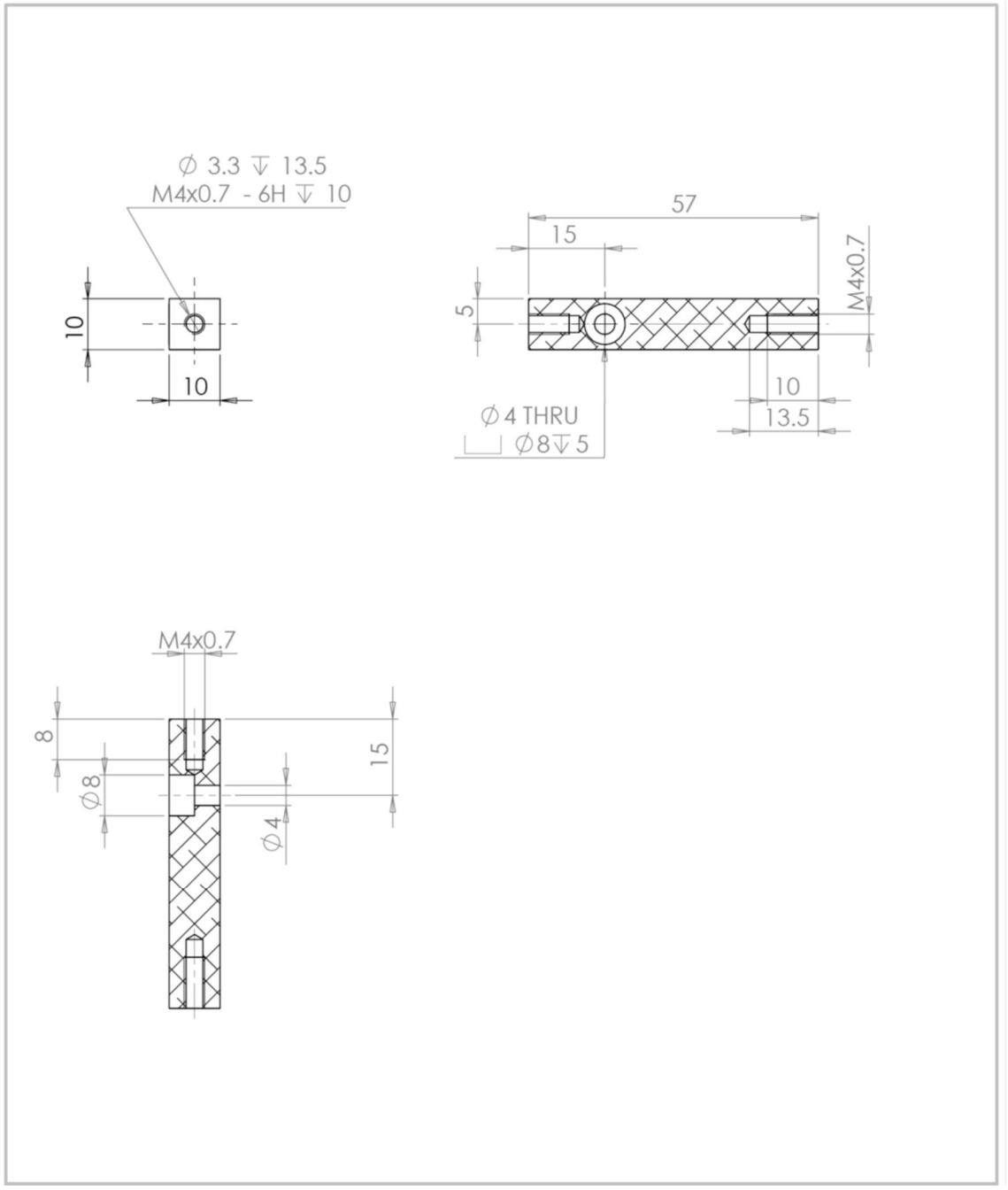

Figure A.5 Support pillars of the module (4 pieces)

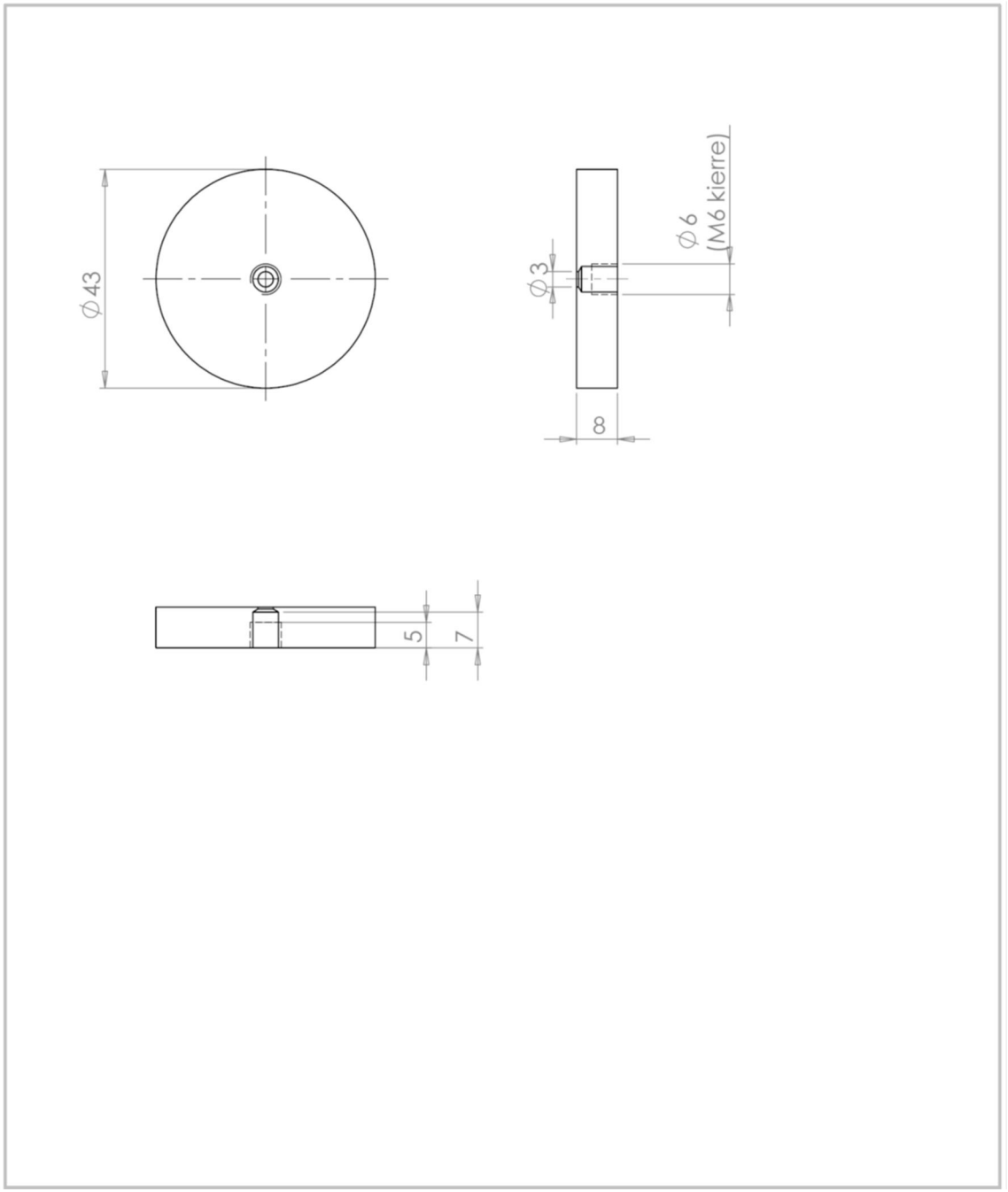

Figure A.6 Table supporting the LED and filtering

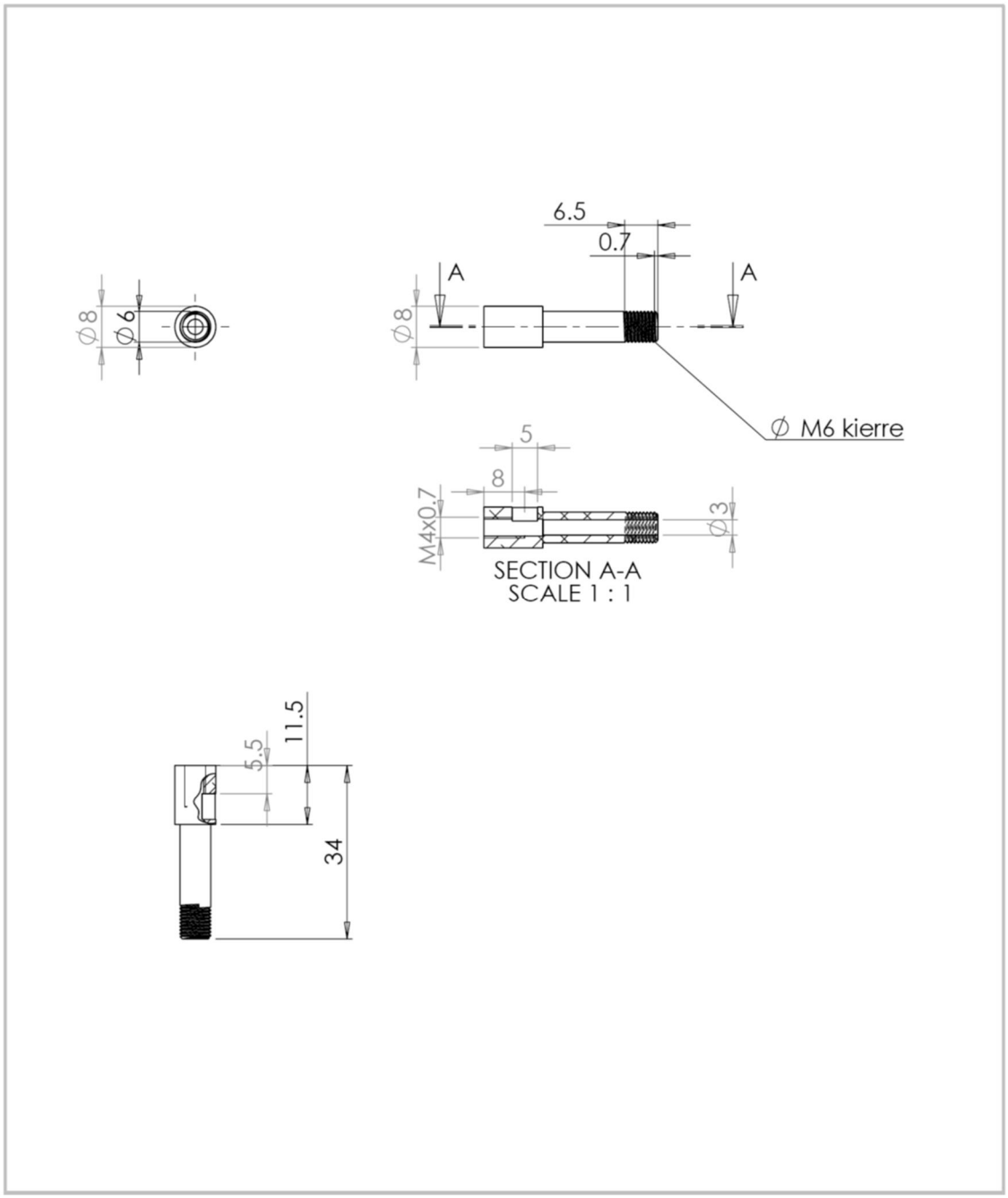

Figure A.7 Horizontal pole supporting the previous component

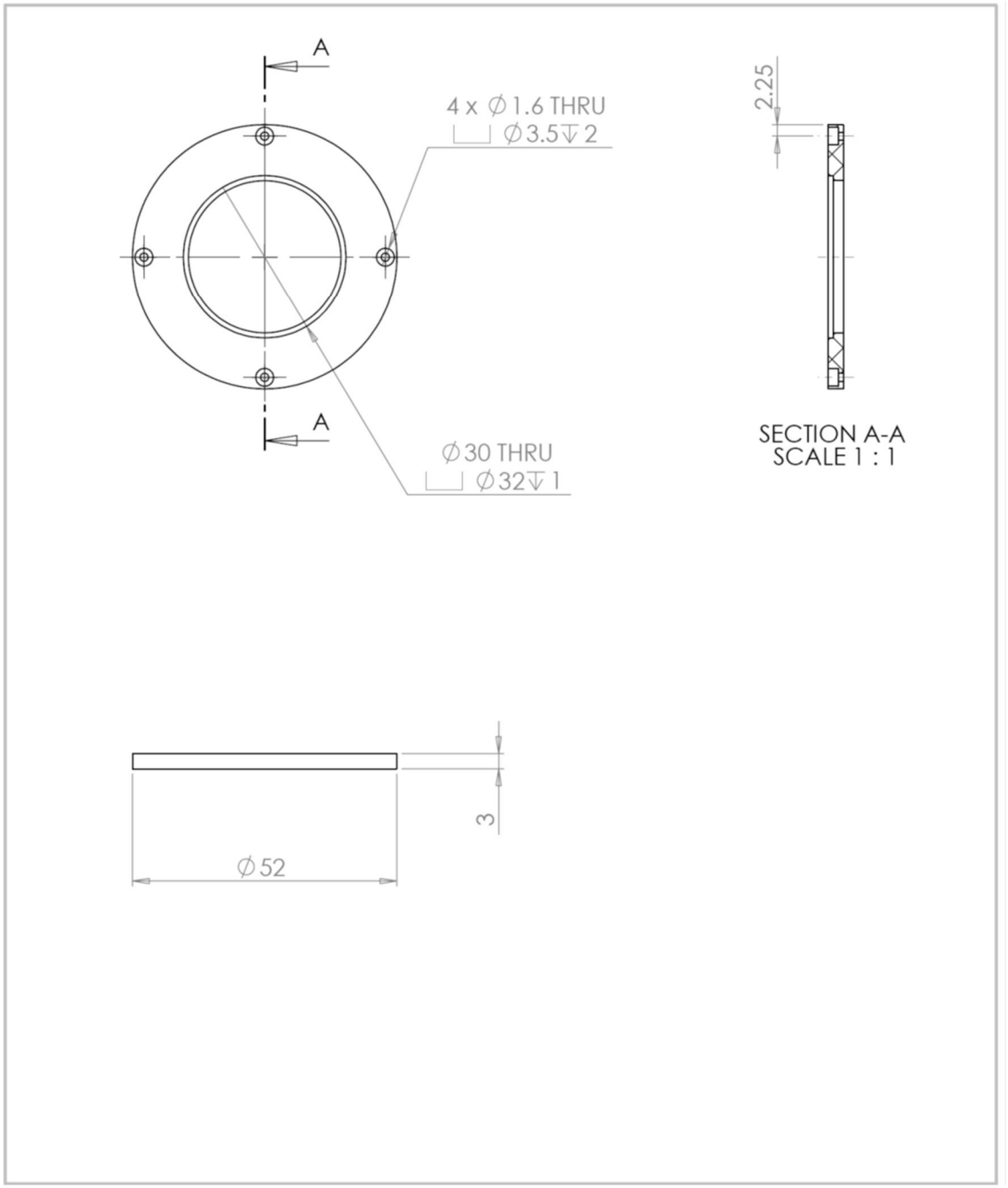

Figure A.8 The top disc of the rotating cylinder. Holds the fiber samples

B. APPENDIX B – MATLAB FUNCTION FOR FIBER SEGMENTATION

The following function was used to perform the fiber segmentation. The image was read in to MATLAB memory and the function was ran with fiber maximum length of 50 (*fibsize* parameter set to 50). The last parameter *thr* was left unused.

```
function [rIm, bgIm, fgIm, sdev, contrast, m1, m2] = findFiberM2(image,
fibsize, thr)
% Finds fibers from sample images using Otsu threshold method
%
% [rIm, bgIm, fgIm, sdev, contrast] = findFiber(image, fibsize)
%
% Parameters:
% fibsize = particles smaller than this will be filtered
%

% Crop coordinates for thresholding of smaller area or any area
figure, imshow(image, [])
title('Please pick a "small" area with fibers and background')
impixelinfo
mask = roipoly(image) ;

%imcrop(image, [a(1) b(1) a(2)-a(1) b(2)-b(1)]) ;
cIm = uint8(double(image).*double(mask)) ;
close all
figure, imshow(cIm)

%% OTSU thresholding of whole image by parameters from cropped area
tlev = graythresh(cIm(find(mask))) ; % calculates Otsu threshold
thr = tlev ;
tIm_p = im2bw(cIm, thr) ; % performs Otsu thresholding

% Same for the whole image
tIm = im2bw(cIm, thr) ;

%% Removes any smaller particles than fibsize parameter
clIm = removeTrash(tIm, fibsize) ;
figure, imshow(clIm, [])
title('Cleaned thresholded image')
rIm = clIm ;

%% Morphological closing of the thresholded image to filter small particles
MIm = bwmorph(rIm, 'close') ;
figure, imshow(MIm, [])
title('Morphologically closed thresholded image')
```